

A Comprehensive Machine Learning Framework for Micromobility Demand Prediction

Omri Porat^{1*}, Eran Ben-Elia², and Michael Fire³

Abstract

Dockless e-scooters, a key micromobility service, have emerged as eco-friendly and flexible urban transport alternatives. These services improve first- and last-mile connectivity, reduce congestion and emissions, and complement public transport for short-distance travel. However, effective management of these services depends on accurate demand prediction, which is crucial for optimal fleet distribution and infrastructure planning. While previous studies have focused on analyzing spatial or temporal factors in isolation, this study introduces a framework that integrates spatial, temporal, and network dependencies for improved micromobility demand forecasting. This integration enhances accuracy while providing deeper insights into urban micromobility usage patterns. Our framework improves demand prediction accuracy by 27–49% over baseline models, demonstrating its effectiveness in capturing micromobility demand patterns. These findings support data-driven micromobility management, enabling optimized fleet distribution, cost reduction, and sustainable urban planning.

Keywords

Micromobility, Urban transportation, Last/first mile, Dockless vehicles, E-scooter, Demand prediction, Spatial features, Temporal features, Municipal organizations, Machine Learning

¹Department of Information Systems Engineering, Ben-Gurion University of the Negev, Beer Sheva, Israel

²Department of Information Systems Engineering, Ben-Gurion University of the Negev, Beer Sheva, Israel

³Department of Environmental, Geoinformatic & Urban Planning, Ben-Gurion University of the Negev, Beer Sheva, Israel

*Corresponding authors: omriporat@post.bgu.ac.il, benelia@bgu.ac.il, mickyfi@bgu.ac.il

1. Introduction

The growing adoption of micromobility, particularly e-scooters [1], as a flexible [2], and sustainable [3, 4] transportation solution is reshaping urban mobility [5]. E-scooters offer a promising solution for short-distance travel [6]. They can help reduce traffic congestion, lower emissions [7], and address first and last-mile connectivity challenges [8]. In cities like Tel Aviv, e-scooters are integral in urban mobility [9], reducing short car trips and complementing public transport [10].

Accurately predicting e-scooter demand remains a critical challenge [11] for effective micromobility management [11]. It is vital for fleet management, ensuring e-scooter availability [12], and infrastructure planning [13]. Micromobility demand is highly dynamic and influenced by complex interactions among spatial, temporal, and network-related factors [14, 15]. Spatial factors [16], such as proximity to public transport hubs [17, 18], bike lanes [19], and land-use patterns [20, 21], significantly impact micromobility demand, while temporal factors such as weather conditions [22, 23], time of day [24], and special events [25] influence demand. Additionally, the urban network structure [26, 27, 28], such as centrality [29], community structure [30], size, and density [31] significantly influences e-scooter demand. Prior research enhances our understanding of the elements influencing e-scooter usage and offers valuable insights into the

demand and factors affecting e-scooter usage.

Prior studies have employed time-series models, such as Prophet [32],¹ or LSTM-TPA (Temporal Pattern Attention) [33], to forecast micromobility demand [34, 30]. However, these models primarily capture temporal trends and fail to account for spatial dependencies. Similarly, spatial machine learning (GeoML) models struggle to capture temporal patterns [35]. Moreover, GeoML and Time-Series models do not incorporate network structure [36].

This study proposes a model that integrates spatial, temporal, and network-based features to improve predictive accuracy. We present a novel machine-learning framework that integrates spatial, temporal, and network features to enhance e-scooter demand prediction in urban settings. (see Section 5).

Our methodology follows a four-phase process designed to adapt to diverse urban environments. The first phase involves data collection *Data partitioning and preprocessing* across three main categories: (a) *Temporal Information* - This includes standardized temporal data such as weather conditions, holiday schedules, public events, economic indicators, and mobility trends; (b) *Spatial information*- This category includes standardized GIS-based spatial data, such as public transport networks, land use patterns, and sociodemographic information; (c) *Network Information* - We gathered, standardized, and converted e-scooter usage data into a network

¹Prophet [32] - a time-series forecasting tool that handles seasonal patterns, missing data, and external regressors.

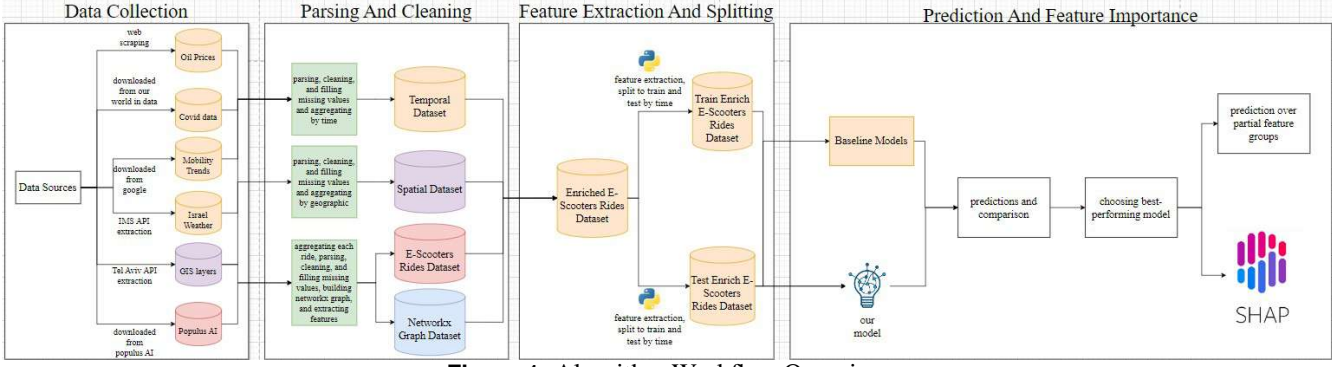


Figure 1. Algorithm Workflow Overview

format. In this representation, the nodes symbolize geographic areas, the edges depict the direct links between these areas, and the weights of the edges reflect the volume of e-scooter trips occurring between them.

The second phase involves extracting and processing features from each data category to prepare inputs for model training. The feature extraction process encompasses three main data categories. Temporal feature extraction involves aggregating data into time-based features to capture seasonal patterns and trends in micromobility usage. Spatial feature extraction involves analyzing patterns across multiple levels—from macro-level (quarters) to micro-level (blocks)—by calculating metrics such as density and proximity using GIS layers. Network analysis involves representing e-scooter trips as a time-dependent directed graph. We analyze the e-scooter network on three levels: (1) Node level—measuring area connectivity using centrality metrics; (2) Edge level—analyzing trip patterns between geographic regions; (3) Graph level—assessing overall network connectivity.

The third phase focuses on developing and evaluating a demand prediction model (see Section 3.3) that integrates temporal, spatial, and network features. Our model combines a time series model to capture temporal patterns and a machine learning ensemble algorithm. We compare our algorithm to several baseline algorithms that use temporal or spatial features. For each algorithm, we evaluate performance using multiple metrics such as Mean Average Error (MAE) and Root Mean Squared Error (RMSE).

Lastly, to interpret our model predictions, we conducted *Feature Analysis* using Explainable AI techniques, such as SHapley Additive exPlanations (SHAP) [37]. SHAP values quantify each feature’s contribution to the model’s predictions, identifying key factors influencing e-scooter demand. This approach provides insights into the contributions of spatial, temporal, and network features, improving interpretability and understanding of the model’s results.

We conducted a large-scale experiment to evaluate our proposed methodology. We used real-world e-scooter data from Tel Aviv provided by Populus AI. It contains approximately 16 million rides (April 2020 to February 2023). We integrated six additional data sources, such as GIS layers, Google Mo-

bility Trends, Energy Prices, and Weather data. In total, we employed 341 features - 238 spatial features, 86 temporal features, and 17 network features. (see Table .1). We aggregate the data across multiple spatial and temporal levels. We subsequently implemented a temporal cut-off method to avoid data leakage. We then used seven different prediction models for comparative analysis and found the best-performing model.

The fully integrated model demonstrated a 27–49% reduction in MAE compared to baseline feature subsets (see Section 5), underscoring the predictive advantage of combining spatial, temporal, and network features. Notably, the inclusion of network centrality metrics contributed the most significant improvement in forecasting accuracy. Our analysis indicates that our model reduced Mean Absolute Error (MAE) by 66-91% compared to the state-of-the-art baseline time series model (see Section 5). Furthermore, our model significantly outperformed baselines relying on individual feature types, reinforcing the importance of integrating spatial, temporal, and network features. These results confirm our model’s ability to capture seasonal trends and improve the accuracy of micromobility demand predictions (refer to Section 5). It demonstrates the significance of integrating diverse features to achieve precise demand forecasting for micromobility solutions.

We assessed the performance of our best-performing model by using only certain groups of features. There are varying degrees of improvement based on the specific types of features included in the evaluation. Specifically, our model, using temporal and network features, improved prediction accuracy by 2-21% compared to network, spatial, and temporal features, 34-63% compared to spatial and temporal features, and 19-39% compared to network and temporal features.

Our results indicate that network features, particularly centrality measures, were the most influential predictors of micromobility patterns in our model (see section 5). SHAP analysis identified node degree and path length as key predictors of e-scooter demand, indicating that areas with higher connectivity within the urban mobility network exhibit greater adoption of micromobility services. It suggests that well-integrated road networks play a vital role in shaping e-scooter usage patterns. These findings underscore the critical role

that urban network structure plays in shaping e-scooter usage patterns.

The remainder of this paper is structured as follows: Section 2 reviews related work on e-scooter ride patterns, feature selection, and machine learning approaches. Section 3 We 3, and the experimental framework 4. Section 5 presents results and performance comparisons with baseline models. Section 7 discusses implications, limitations, and conclusions. Finally, Section 7 outlines directions for future research.

2. Related Work

This section reviews prior research on micromobility demand prediction, focusing on spatial, temporal, and network-based factors, as well as machine learning approaches. First, we analyze temporal and spatial patterns affecting micromobility demand (see Section 2.1), such as weather conditions, land use and connectivity. Second, we explore machine-learning approaches in micromobility, focusing on time-series models (Section 2.2). Finally, we review SHAP and Prophet and their role in understanding micromobility behavior (Section 2.3).

2.1 Spatial, Temporal, and User-Related Factors in Micromobility Demand

Understanding e-scooter demand requires analyzing spatial and temporal factors that shape micromobility usage. Prior studies have examined these influences in diverse urban settings, providing insights into demand fluctuations [9, 38, 39]. Studies indicate that road infrastructure significantly influences e-scooter adoption, with key factors including cyclist comfort, road maintenance, and route flexibility. For example, Feng et al. [40] found a strong correlation between e-scooter adoption and cyclist comfort ratings in Austin, Texas, suggesting that well-maintained cycling infrastructure encourages usage. Similarly, Lazarous et al. [41] showed that dockless e-scooters outperformed e-bikes in less populated areas in San Francisco, demonstrating user preferences for more flexible transportation modes. Rodriguez et al. [42] showed that better-maintained road infrastructures in Puerto Rico significantly increase e-scooter adoption. These findings demonstrate the vital role of infrastructure in shaping micromobility usage patterns. User demographics and the interplay with other transportation modes are equally important. Liao and Correia, Sophia et al., Bretones and Orio, and Christoforou et al. [43, 44, 45, 46] found that e-scooter users were predominantly young, educated, and affluent. In central Austin, Caspi et al. In Taipei, Liu and Lin [47] demonstrated similarities in travel time and distance but differences in high-demand areas and rush hour usage. Taipei, Liu and Lin [47] demonstrated similarities in travel time and distance but differences in high-demand areas and rush hour usage.

The presented studies discuss different transportation modes, user profiles, and road infrastructure as predictors for e-scooter usage. While these studies provide valuable insights, they often focus on spatial or temporal features, without integrating

them. Moreover, they overlooked network features, which are vital in micromobility demand [13].

Temporal factors, such as weather and fuel prices, significantly affect micromobility demand. Mehzabin Tuli et al. [48] developed a regression model incorporating these variables to predict e-scooter demand patterns. Among temporal factors, weather conditions, such as rainfall and temperature, significantly influence micromobility usage patterns. Noland [49] showed that rain and cold temperatures significantly influenced micromobility usage. Also, Xin et al. [50] showed that the pandemic led to fewer trips and fewer rush-hour rides while long-duration trips increased. Integrating these diverse findings provides a comprehensive view of the main factors influencing micromobility usage patterns.

While prior research has explored these factors separately, an integrated approach that considers spatial, temporal, and network features is essential for improving predictive performance.

2.2 Machine Learning Approaches for Micromobility Demand Prediction

Building on these demand-influencing factors, researchers have explored machine-learning techniques for micromobility prediction, ranging from classical regression models to deep-learning approaches.

2.2.1 Classical Machine Learning Approaches

Several studies have applied traditional machine learning techniques, including regression [24, 25] and ensemble models [22, 51], to forecast micromobility demand. These models often capture correlations between external features, such as weather, land use, sociodemographic features, and micromobility trip volumes. Early studies applied regression models to predict micromobility demand based on spatial or temporal features. For instance, Wang et al. [52] applied Random Forest (RF) and Gradient Boosting Machines (GBM) to predict e-scooter demand in Beijing. Additionally, Maren Schieder [53] demonstrated the effectiveness of RF models for bike-sharing demand prediction in London.

More recent studies, such as Zuniga-Garcia et al. [54], applied XGBoost to predict e-scooter demand in Austin, Texas and demonstrated enhanced accuracy compared to linear models in capturing non-linear dependencies. Lin et al. [55] developed an adaptive XGBoost model for shared bicycle demand prediction in Shanghai, combining both weather and urban morphology features.

Despite their advantages, classical ML approaches assume feature independence [56], which is problematic for micromobility demand data [19, 57] due to inherent spatial [58] and temporal [59] autocorrelations. Short-term demand fluctuations and seasonal effects which necessitate more sophisticated modeling techniques.

2.2.2 Temporal Machine Learning Approaches

Due to the seasonal and short-term fluctuations in micromobility demand, researchers have explored time-series forecasting

techniques for improved prediction. Some of the methods include Prophet [32], LSTMs [60], and GRU-based (Gated Recurrent Units) architectures [61].

Wang et al. [34] applied Prophet, an open-source tool used for forecasting time series data, to predict micromobility usage in New York City, achieving enhanced results than traditional time series approaches by combining holidays, events, weather conditions, and mobility trends. However, Prophet struggles to model non-linear interactions and lacks the ability to capture spatial dependencies in micromobility demand.

Deep learning approaches, mainly LSTM (Long Short-Term Memory) networks, capture long-term and short-term seasonality. For example, Yu et al. [33] developed an LSTM-TPA (Temporal Pattern Attention) model to forecast e-scooter demand in Chicago, demonstrating its ability to capture short-term fluctuations during special events and holidays. The LSTM provided superior accuracy to traditional ML models by learning complex temporal dependencies.

While time-series models (Prophet, LSTM, GRU) effectively capture temporal dependencies, they fail to incorporate spatial relationships and network structures—key elements influencing micromobility demand.

Despite advancements in spatial and temporal micromobility forecasting, existing models overlook the impact of network connectivity on demand patterns. This study addresses this gap by integrating spatial, temporal, and network-based features into a unified machine-learning framework.

2.3 Time Series and Model Explainability Tools

This study utilizes Prophet [32] for time-series forecasting and SHAP [37] for model explainability. Prophet captures seasonal trends in micromobility demand, while SHAP quantifies the influence of individual features on model predictions.

Prophet [32] is a general-purpose time-series forecasting model for micromobility demand prediction. Wang et al. [52] used Prophet to forecast e-scooter demand in New York City, integrating weather conditions and public holidays as key predictors. Similarly, Hernandez et al. [62] used Prophet to analyze micromobility seasonality in Chicago, capturing daily commuting patterns and weekend usage distributions.

SHAP (SHapley Additive Explanations) [37] enhances model interpretability by assigning importance scores to individual features, explaining their contribution to predictions. Shalit et al. [63] used SHAP to identify prominent features imputing missing boarding stops in smart card data. In micromobility research, Zuniga-Garcia et al. [54] applied SHAP to analyze e-scooter demand in Austin. Their findings highlighted bike lane density and public transport proximity as primary influencing factors. Similarly, Shahal et al. [64] employed SHAP to quantify weather-related influences on e-scooter demand in Tel Aviv, reinforcing the role of environmental factors in micromobility forecasting.

3. Methods

This study proposes a machine-learning framework to predict micromobility demand across different geographic scales. The methodology follows a two-stage approach: (1) model development and (2) experimental evaluation. We develop a generalized machine-learning model for micromobility demand prediction, ensuring adaptability across different urban environments. Our framework consists of four key steps: (1) data preprocessing, (2) feature engineering, (3) model construction, and (4) model evaluation. Each step is detailed in the following subsections.

3.1 Data Preprocessing

Micromobility ride data is collected from municipal agencies, service providers, and open data portals. Each record includes trip origin, destination, start and end times, and ride duration. We first clean the data by removing trips with empty fields and removing abnormal trips, which are trips with a duration of less than t_{min} seconds or higher than t_{max} .

We aggregate the ride data based on a temporal variable, T_{scale} . The variable represents different time scales, such as hour, day, or month. This temporal aggregation allows for the examination of trends at varying levels of granularity. That allows us to analyze short-term fluctuations and long-term trends in micromobility demand.

Spatial aggregation S_{level} is performed at multiple levels, ranging from large city quarters to fine-grained hexagonal grid units. The multi-scaled approach guarantees that predictions can adjust to macro and micro changes and different urban planning requirements. The micromobility dataset is enriched with external data sources to incorporate broader urban context. These sources include:

Temporal Data. We include weather conditions, such as temperature, wind speed, humidity, and precipitation, as these factors affect micromobility demand. We combine public events and holidays, which can affect micromobility demand. Then, we combine economic indicators, such as daily energy prices, to assess their influence on micromobility adoption. We then add mobility trends, such as residential and transport time, to evaluate their effect on micromobility demand fluctuations.

Spatial Data. Our framework integrates spatial features including urban infrastructure and road networks. These features are extracted from points of interest, public transport hubs, and land use classifications to predict micromobility demand patterns. The list of spatial features with their descriptions is in Table S3. We categorized the spatial features into three geometric types based on their shape: Point Features (P): Elements that represent discrete locations in space, defined by coordinate pairs (x, y) . These include specific points of interest, such as docking and bus stations. Line Features (L): Elements that represent vectors between two or more points, defined by a series of connected coordinates $(x_1, y_1), (x_2, y_2), \dots, (x_n, y_n)$. These features capture paths, such as metro lines and bike lanes. Polygon Features

(A): Elements characterized by closed boundaries that enclose specific areas, represented as a sequence of coordinates, denoted as $[(x_1, y_1), (x_2, y_2), \dots, (x_n, y_n), (x_1, y_1)]$.² These features represent land use zones and districts, such as parks, commercial areas, and residential zones.

Network Data. We model the micromobility ride network as a time-dependent directed graph $G_t^s = (V_t^s, E_t^s, W_t^s)$, where V_{st} represents nodes (geographic areas) at time t and spatial division s , and edges E_t^s capture ride connections weighted by trip volume W_t^s . Each node represents a geographic area. E_t^s is the set of directed edges at time t , and spatial division s , where an edge (v_i^s, v_j^s) exists if there are recorded micromobility trips from area v_i^s to v_j^s . W_t^s is the set of edge weights at time t and spatial division s , w_{ij}^s represents the volume of trips between areas v_i^s to v_j^s . The network uses origin-destination pairs from the micromobility ride data, providing insight into connectivity patterns and centrality. We join the data sources with micromobility rides data. We then perform data normalization using min-max scaling and filling in missing values to ensure we can perform feature extraction and model training over the data.

3.2 Feature Engineering

In this study, we predict the micromobility flow between spatial regions at a given time, represented as the weight of an edge in the time-dependent network. We integrate the micromobility rides dataset with the temporal, spatial, and network attributes to predict these flows. We categorize and compute the extracted features into spatial, temporal, and network features:

Temporal Data (see Table S4) We integrate for each T_{scale} and S_{level} temporal datasets to enhance micromobility demand predictions. Data acquisition from open APIs and government portals enables the extraction of key features, which are categorized as follows:

- *Mobility Trends:* We gather historical data from Google Mobility Trends to analyze how much time people spend in different locations, including workplaces, residences, transportation, and recreational areas. We use mobility data that precedes our prediction periods to avoid data leakage. These insights help us understand the overall patterns and dynamics of transportation.
- *Special Events:* We extract features such as weekdays/weekends and holidays. Those features can capture temporary demand hotspots.
- *Energy Prices:* We extract features, including WTI and Brent oil prices, which precede our prediction periods. These prices have the potential to influence the overall demand for micromobility services.

²Polygon is a closed geometric shape formed by connecting a sequence of points (vertices) in a plane. It is mathematically represented as $[(x_1, y_1), (x_2, y_2), \dots, (x_n, y_n), (x_1, y_1)]$, where each (x_i, y_i) represents the coordinates of a vertex, with the first point repeated at the end to close the shape.

- *Weather Conditions:* We extract features such as temperature, wind speed, rain, and humidity forecast for our prediction periods. Those features can affect overall micromobility demand.
- *Seasonality Patterns:* We include seasonality-based features from Prophet to enhance prediction accuracy that capture periodic demand fluctuations, such as holiday effects. It captures patterns from our temporal data and adds to the final dataset.

Spatial Features (see Table S3): We divide the GIS layers into three primary feature types: Point-based, Line-based, and Polygon-based features. Each category provides spatial attributes that influence micromobility patterns. The extracted features are detailed as follows:

- *Point-Based Features:* We use point-based features such as e-bike stations, e-scooter docking points, public transportation stops, train stations, commercial stores, schools, hospitals and government buildings. We determine numerical indicators by calculating the number of facilities within each designated spatial unit for each feature. For instance, if a spatial unit contains three bus stations, we classify it under the feature "number of bus stations." This count-based approach allows us to capture the density and distribution of urban infrastructure within each analysis zone.
- *Line-Based Features:* We use line-based features such as bike lanes, pedestrian paths, highways, main roads, metro lines and bus lanes. We calculate the total length of relevant road segments within each spatial unit for each feature.
- *Polygon-Based Features:* We use polygon-based features such as parks, nature reserves, housing, and commercial areas. We calculate the total area of different land-use categories within each spatial unit for each feature.

Network Features (see Table S5): For each T_{scale} and S_{level} , we extract from the time-dependent directed graph G_t^s network features and divide them into three primary feature types: Node-based, Edge-based, and Network-based. Each category provides attributes that influence micromobility patterns. The extracted features are detailed as follows (see Table S5):

- *Node-Based Features:* We use node-based features such as betweenness centrality [65]³ and degree centrality [66].⁴ We calculate it for each node in the graph.

³Betweenness centrality of a node is the sum of the fraction of all-pairs shortest paths that pass through the node

⁴The degree centrality for a node v is the fraction of nodes connected to.

- *Edge-Based Features:* We use edge-based features such as edge betweenness centrality [65]⁵ and edge connectivity [67]⁶. We calculate it for each edge in the network.
- *Network-Based Features:* We use network-based features such as average degree connectivity [68]⁷ and clustering coefficients [69].⁸ We calculate it for the whole graph.

3.3 Constructing Prediction Model

In this section, we construct a micromobility demand prediction framework based on the extracted features described in Section 3.2. Our approach combines regression-based models with time-series forecasting to enhance prediction accuracy. We used seven machine-learning models to evaluate our model: Decision Tree [70], Elastic Net [71], Lasso Regression [72], Ridge Regression [73], Random Forest [74],⁹ Nearest Neighbors [75], and Prophet [32]. Prophet is a time-series forecasting model designed to capture seasonality, short-term fluctuations, and long-term trends.

Our prediction framework consists of three main steps: data splitting, model evaluation, and feature importance analysis. In data splitting, for each T_{scale} and S_{level} , we apply temporal cut-off¹⁰ to ensure that our evaluation reflects real-world forecasting and prevents data leakage. In model evaluation, we train and evaluate the performance of seven machine learning models using evaluation metrics such as Mean Absolute Error (MAE), Root Mean Squared Error (RMSE), and Mean Absolute Percentage Error (MAPE).

3.4 Feature Group Analysis

After evaluating the seven predictions models with all the features, we then select the best-performing model. Next, we examine the contribution of different feature groups to the model performance.

Additionally, we train and evaluate the best-performing model using three distinct feature groups- spatial features, network features, and temporal features and combine them:

- *Network and temporal features (see Tables S5 and S4) -* Includes network characteristics, such as connectivity and centrality, with temporal attributes, such as mobility trends, energy prices, and holidays.

⁵Betweenness centrality of an edge is the sum of the fraction of all-pairs shortest paths that pass through the edge [65].

⁶The edge connectivity is equal to the minimum number of edges that must be removed to disconnect G or render it trivial. If source and target nodes are provided, this function returns the local edge connectivity: the minimum number of edges that must be removed to break all paths from source to target in G [67].

⁷Compute the average degree connectivity of graph. The average degree connectivity is the average nearest neighbor degree of nodes with degree k [68].

⁸For unweighted graphs, the clustering of a node is the fraction of possible triangles through that node that exist [69].

⁹We ran the models with default values. Then, we ran XGBoost and Random forest with $n_{estimators}$ of 1000

¹⁰Temporal Cut-Off is a point in time used to divide a dataset into training and testing sets

- *Spatial and temporal features (see Tables S3 and S4)* - Includes spatial characteristics, such as public transportation routes, land use, and points of interest, with temporal attributes, such as mobility trends, energy prices, and holidays.
- *Network and spatial features (see Tables S3 and S5)-* Includes network characteristics, such as connectivity and centrality, with spatial characteristics, such as public transportation routes, land use, and points of interest.

Finally, we conduct a feature importance analysis for the best-performing model using SHAP values to identify the most influential features for micromobility demand prediction. The insights can support policymakers in optimizing urban mobility by identifying features and feature groups that influence on micromobility adoption.

4. Experiments

We test the effectiveness of our methodology using real-world e-scooter data from Tel Aviv. This phase involved structured experimentation to assess model performance in a real urban environment.

4.1 Datasets and Data Processing

Datasets. We integrated six datasets, each adding crucial spatial, temporal, or network-based attributes to strengthen our micromobility demand predictions model:

- *E-Scooter Ride Data (Populus AI) [76]* A dataset that comprised approximately 16 million e-scooter trips recorded in Tel Aviv from April 2020 to February 2023, including trip duration, distance, start and end times, and routes.
- *Tel Aviv GIS Data [77]*– A comprehensive dataset that integrates 235 spatial layers of urban infrastructure, public transport centers, and cycling pathways.
- *COVID-19 Data (Our World in Data) [78]* – Global pandemic-related metrics affecting urban mobility. The dataset contains 98 features.
- *Fuel Price Data [79]*– Weekly prices of global oil and gas from 2020 to 2023. The dataset contains two features, WTI prices and Brent prices.
- *Google Mobility Trends [80]* – City-level movement trends across different sectors. The dataset contains 2 features.
- *Weather Data [81]* – Daily temperature, precipitation, and wind speed records from the Israel Meteorological Institute.

After integrating the data from the six datasets, We first cleaned the e-scooter ride dataset by handling missing values and removing trips with a duration of less than 30 seconds or

higher than 2 hours. We chose those trips duration to eliminate outliers or system malfunction. The average micromobility trip in Tel Aviv is between 10-15 minutes.

4.2 Feature Extraction

After integrating the data from the six datasets, We first cleaned the e-scooter ride dataset by handling missing values and removing trips with a duration of less than 30 seconds or higher than 2 hours.

Next, we extracted features by aggregating data across temporal and spatial dimensions to ensure a structured and meaningful representation. We aggregated the data across the three T_{scale} : monthly, daily, and hourly, to capture long-term trends and short-term fluctuations. Later, we performed spatial aggregation over six S_{level} : quarters, subquarters, neighborhoods, city blocks, statistical areas, and hexagonal grids. We have 18 combinations of spatial and geographic levels in total. We categorized the extracted features into three primary types: temporal, spatial, and network features.

Temporal Features (see Table S4) For each T_{scale} and S_{level} , we integrate the external datasets to enhance micromobility demand prediction. The temporal features include:

- *Mobility Trends*: Features that measure fluctuations in visits to different locations in Tel Aviv, including workplaces, residences, transportation hubs, and park areas.
- *Special Events*: We extract features such as weekdays / weekends and Jewish holidays.
- *Energy Prices*: We extract features, including WTI and Brent oil prices in Israel.
- *Weather Conditions*: We extract weather features in Tel Aviv, such as temperature, wind speed, rain, and humidity.
- *Seasonality Patterns*: We include seasonality-based features from Prophet to enhance prediction accuracy that capture periodic demand fluctuations, such as Jewish holiday effects and weekdays prior scale.

The final dataset includes 86 temporal features, all detailed in Table S4.

Spatial Features (see Table S2) For each T_{scale} and S_{level} , we extract spatial features from the GIS layers by dividing the data into three feature types: point-based features - P , line-based features - L , and polygon-based features.

- *Point-Based Features*: We 135 use point-based features such as The number of Tel-O-Fun docking stations, Dan and Egged bus stations, Kindergartens, and Israel Rail stations, within each S_{level} .
- *Line-Based Features*: We use 31 line-based features such as the length of Tel-O-Fun lanes, highways, M1-M3 light train (metro) lines and bus lanes within each S_{level} .

- *Polygon-Based Features*: We use 72 polygon features such as the total area of parks and commercial areas within each S_{level} .

We extract 238 spatial features, provided in Table S3.

Network Features (see Table S5) we construct the time-dependent directed network G_t^s .¹¹ We extracted 17 network features, categorized as follows:

- *Node-Based Features*: We use node-based features such as betweenness centrality and calculate it for each node in the network, such as, betweenness centrality of Yad Eliyhau Neighborhood.
- *Edge-Based Features*: We use edge-based features such as edge betweenness centrality and edge connectivity and calculate it for each edge in the network, such as the connectivity between the the Ramat Aviv and Nave Shaan neighborhoods.
- *Network-Based Features*: We use edge-based features such as average degree connectivity and clustering coefficients and calculate it for the whole network.

In total, we used 341 features- 238 spatial features, 86 temporal features, and 17 network features.

4.3 Model Evaluation

We split the dataset into training (2020–2022) and testing (2022–2023) subsets using a temporal cut-off approach, as described in Section 3.3.

We trained the best-performing model in three distinct feature sets:

- *Network and Temporal Features*: provided in Tables S4 and S5.
- *Spatial and Temporal Features*: provided in Tables S2 and S4.
- *Network and Spatial Features*: provided in Tables S2 and S5.

Lastly, we applied SHAP-based feature importance analysis to interpret the key factors driving micromobility demand (see Figure 1).

5. Results

In this section, we present the experiment results. First, we present the e-scooter ride data and network characteristics with temporal and spatial analysis. Second, we present our model results and best-performing model results over partial feature groups and SHAP analysis results. The e-scooter

¹¹We used NetworkX [82] - a Python package for the creation, manipulation, and study of the structure, dynamics, and functions of complex networks. Nodes represented geographic areas within specific time frames, while edges represented the number of trips between nodes, with weights capturing trip volumes

rides dataset includes approximately 16 million rides, with an average trip duration of 14 minutes and an average distance of 2.5 kilometers per trip, from April 2020 to February 2023. After removing incomplete records and trips shorter than 30 seconds or longer than 2 hours, the data set remains with 15.4 million rides.

We split the dataset into training (April 2020 - October 2022) and testing (November 2022 - February 2023) using a temporal cut-off approach. The train data contains 13.8 million trips, while the test data contains 1.6 million.

Then, we constructed a time-dependent directed network G_t^s , for each T_{scale} and S_{level} , where the network structure is T_{scale} invariant. The following table describe the network property for each S_{level} (see Table S1).

Table S1. Network statistics at different spatial levels

Level	Nodes	Edges	Average Weights
Quarters	9	81	14,214.16
Subquarters	31	914	1,259.68
Neighborhoods	70	3,359	342.76
Statistical Area	172	20,029	57.48
City Blocks	1,205	45,910	25.08
Hexagonal Grid	6,854	251,940	4.57

We conducted a temporal analysis of the e-scooter hourly, weekly, and yearly demand (see Figure 2): We observed peak demand between 8:00 to 9:00 AM and 5:00 to 6:00 PM, aligning with commuter travel times. Minimal usage between midnight and 5:00 am, suggesting that e-scooters are for daily commute rather than late-night travel.

Then, we analyzed weekly demand in Tel Aviv on weekdays in June 2022.

We notice a higher demand on weekdays, especially Thursdays, correlates with work commute behavior. We observe a decrease in Saturdays when public transport is unavailable.

We analyze the total demand for e-scooter in Tel Aviv in 2022. We notice a significant demand increase in the summer (June–August). Winter decline, demonstrating high weather sensitivity. These insights indicate that e-scooter operators could dynamically adjust fleet availability in response to peak hours, weekdays, and seasons.

We conducted a spatial analysis of the e-scooter rides over three divisions- quarters, statistical areas, and blocks. Figure 2 presents the micromobility demand by quarters in June 2022. The highest demand is in central city quarters (quarter 3 and quarter 5), characterized by commercial density and transport hubs. It also presents the demand for micromobility by statistical areas in June 2022. The highest demand is in statistical areas 81 and 116, which have higher average income and younger population, and presents the micromobility demand by blocks in June 2022. The highest demand is in Blocks 246, 408, 1, and 831, which are near the coast.

We trained several machine-learning models and evaluated their performance using MAE (Mean Absolute Error), MAPE (Mean Absolute Percentage Error), and RMSE

(Root Mean Squared Error) across different T_{scale} and S_{level} . Among all machine-learning models, the XGBoost regressor¹² demonstrated the best results (see Figures S4 and S5) in almost all cases with different T_{scale} and S_{level} , for each evaluation metric. We selected the best-performing regressor based on the importance of features and feature groups, utilizing partial feature groups and SHAP analysis.

We performed a partial feature group analysis over the best-performing model (XGBoost) for each T_{scale} and S_{level} and evaluation metric (see Table S7). In Figure 2 and S7, we have a partial feature groups comparison for the best-performing model. In this analysis, network features had the highest impact on prediction accuracy, followed by temporal and spatial features.

Lastly, we performed a SHAP analysis over the best-performing model (XGBoost). Figures S8 show the 10 most prominent features for prediction, for different T_{scale} and S_{level} . The SHAP analysis revealed that previous count, shortest path length, degree, centrality and strength were the most significant factors influencing e-scooter demand. Among temporal features, the most influencing features were previous count, previous weather description, and total cases.

6. Discussion

In this study, we successfully developed a general micromobility demand prediction model and tested the model in Tel Aviv. Our approach integrates machine-learning algorithms with spatial, temporal, and network features. Our research revealed that applying machine learning techniques and integrating network features enhance micromobility demand predictions, which can benefit policymakers and micromobility providers.

According to the results, We can infer the following conclusions:

The machine-learning algorithm generates a generic model applicable to different cities since we extracted diverse generic features (see Section 3.2). We improved demand predictions by extracting features from each network G_t^s that efficiently represent the network topology. The demand areas are inherently imbalanced, as seen in Figure 2. Peripheral regions exhibit lower demand, suggesting the potential to expand the accessibility of micromobility. Coastal districts (e.g., Blocks 246, 408, 1, and 831) and commercial zones exhibit high e-scooter usage due to their cycling infrastructure, proximity to the city center, and high pedestrian activity, suggesting the potential to expand micromobility adoption in those areas. Areas with higher income and younger populations (e.g., Statistical Areas 81 and 116) demonstrate higher adoption rates, aligning with prior studies on demographic influences on micromobility usage. Various feature types—spatial, temporal, and network-based—allow for a more comprehensive representation of factors influencing micromobility usage. Our framework integrates multiple geographic scales and time

¹²We ran the XGBoost with the following configuration: number of estimators equals to 2000, learning rate of 0.1, max depth of 5, and hist as tree method

frames, capturing demand patterns from quarters to blocks level and from monthly to hourly timeframes. Our method requires a micromobility rides dataset, and integrating network and temporal features enhances the predictions.

Second, our model, applying the XGBoost algorithm, provided the highest performance for each T_{scale} and S_{level} , with 27–49% improvement in predictive accuracy compared to existing approaches and enhanced prophet predictions by 66–91% (see Figure S5). The network and temporal features significantly boost model performance.

We analyze the best-performing model (XGBoost) by running partial feature groups to understand each feature group's contribution to the prediction accuracy. The partial feature groups were spatial, temporal, network, spatial and temporal, network and spatial, network and temporal, and all feature groups. Our results show that the combination of network and temporal features outperformed each partial feature group, including groups with spatial, temporal, and network features. We aggregated the number of facilities, surface areas, and total line lengths within each spatial division for each spatial feature. However, this approach may not fully capture the spatial context. Future research can enhance spatial feature extraction by developing more sophisticated and generalizable methods to encode spatial context.

We then evaluated each feature group separately to find the most influential feature group. Network features are the most influential, followed by temporal features and spatial attributes (see Figure S7). The network features are derived from the e-scooter rides dataset and capture key aspects of the network, such as degree and centrality, which are critical for demand prediction. The temporal features, such as weather conditions, are dynamic in time and reflect real-time fluctuations in demand. However, the spatial features we chose, such as park total area, metro line length, and buildings, might be less effective predictors of e-scooter demand since they are static in time and may not capture the spatial context.

Spatial features demonstrated the weakest influence over predictions. It may be because the selected spatial features (see Table S2) are less relevant to e-scooter movement relative to connectivity, centrality, and weather.

The findings suggest that network features, such as centrality and connectivity, are critical in capturing micromobility patterns, particularly when combined with temporal factors, such as weather and special events, likely because temporal patterns introduce dynamic behavioral insights that complement the network features. We achieve high prediction accuracy using network and temporal features, 103 features from the 341. However, the result is specific to the Tel Aviv network, and outcomes may differ in other cities with different infrastructures.

From the SHAP values (see Figure S8), we notice that the characteristics of the network, mainly the centrality of the distance and the proximity, are the most influential, which means that accessibility within the micromobility network is critical in the prediction of demand. For temporal features, weather-

related factors such as temperature and rainfall significantly affect usage patterns, similar to prior studies.

However, our study has certain limitations. The model relies on historical micromobility data, which can produce biases and reduce model accuracy if the mobility patterns change over time. Although our model is general, we evaluated it in Tel Aviv. Cities with different infrastructures might show different demand patterns and require feature tuning. Generalizing the model to distinct cities can improve the robustness of the model and refine the predictions. We mainly focused on spatial, temporal, and network-based features. Other factors, such as user behavior and demographics, can influence micromobility demand, and integrating them can enhance model accuracy. Our study relies on open-source and municipal datasets, which can contain missing values, inconsistencies, or biases. The micromobility data may not always be accessible. Those factors can affect the model's predictions significantly.

7. Conclusions

This study presents a machine-learning-based methodology to forecast micromobility demand, integrating spatial, temporal, and network-based features. Our method follows a four-step process: data collection (see Section 3.1), feature extraction (see Section 3.2), constructing a prediction model (see Section 3.3), and model evaluation and analysis (see Section 3.4). We used various regression-based models to predict e-scooter demand, chose the best-performing model, and performed partial feature group analysis and SHAP to find the most influential features and feature groups.

We applied our framework to e-scooter demand prediction in Tel Aviv, Israel and evaluated the performance across different S_{level} and T_{scale} . Using our method over different regressors, over the spatial, temporal, and network features, we notice that the XGBoost model outperforms the models for each S_{level} and T_{scale} , reducing the second-best model's MAE and RMSE by 27–49%. We then chose the best-performing model (XGBoost) and evaluated it over partial feature groups. Interestingly, XGBoost models trained on temporal and network features outperformed models trained on all three feature groups. The SHAP analysis determined that the most influential network features were degree, strength, shortest path length, and weather conditions among temporal features.

There are many potential directions for future research. Micromobility providers and policymakers can derive valuable insights using our method. Applying our methods in cities such as Los Angeles, Tokyo, and Amsterdam is a promising research direction to improve generalization. Future studies can expand to other micromobility modes, such as e-bikes and segways, enhancing urban mobility planning. Each mode has unique operational constraints, and an integrated dataset can enable micromobility providers to coordinate between different micromobility modes and promote micromobility usage. Future studies can enrich the data to provide a more comprehensive understanding of micromobility trends. Com-

binning datasets on special events, traffic conditions, and socio-economic factors can improve micromobility demand predictions.

We can test different machine learning techniques to enhance predictive accuracy, as mentioned in Section 2.2.2. Applying spatial models like Geographically Weighted Regression [83] can address localized variations, while Graph Neural Networks [84] and Spatiotemporal Graph Neural Networks [85] offer improved forecasting by capturing both spatial dependencies and temporal trends.

Finally, we hope to extend this research by developing a generic, flexible, open-source framework to forecast micromobility demand. This framework would enable researchers and practitioners to change and adjust the parts of our method and use different algorithms for each part, enabling further exploration and understanding of micromobility demand.

8. Acknowledgments

This research was supported by Dr. Ethel Friedmann Fund. We thank Tel Aviv Municipality and Populus AI for providing the data for this study. In addition, while drafting this article, we used ChatGPT, Claude and Grammarly for slight editing according to necessity.

References

- [1] Michael McQueen, Gabriella Abou-Zeid, John MacArthur, and Kelly Clifton. Transportation transformation: Is micromobility making a macro impact on sustainability? *Journal of Planning Literature*, 36(1):46–61, 2021.
- [2] Zong Wei Goh and Nik Hisyamudin Muhd Nor. Design of mobile scooter to increase flexibility and user friendliness. *Research Progress in Mechanical and Manufacturing Engineering*, 3(1):988–997, 2022.
- [3] Elliot Fishman and Susan Shaheen. Bikesharing’s ongoing evolution and expansion. *Transportation Research Record*, 2021.
- [4] Luyu Liu and Harvey J Miller. Measuring the impacts of dockless micro-mobility services on public transit accessibility. *Computers, Environment and Urban Systems*, 98:101885, 2022.
- [5] Rusul L. Abduljabbar, Sohani Liyanage, and Hussein Dia. The role of micro-mobility in shaping sustainable cities: A systematic literature review. *Transportation Research Part D: Transport and Environment*, 92:102734, 2021.
- [6] Rusul L Abduljabbar, Sohani Liyanage, and Hussein Dia. The role of micro-mobility in shaping sustainable cities: A systematic literature review. *Transportation research part D: transport and environment*, 92:102734, 2021.
- [7] H  lie Moreau, Lo  c de Jamblinne de Meux, Vanessa Zeller, Pierre D’Ans, Coline Ruwet, and Wouter MJ Achten. Dockless e-scooter: A green solution for mobility? comparative case study between dockless e-scooters, displaced transport, and personal e-scooters. *Sustainability*, 12(5):1803, 2020.
- [8] Natalia Zuniga-Garcia, Mauricio Tec, James G Scott, and Randy B Machemehl. Evaluation of e-scooters as transit last-mile solution. *Transportation research part C: emerging technologies*, 139:103660, 2022.
- [9] Ofer Shahal, Itzhak Benenson, Aleksey Ogulenko, and Arik Talor. Towards a sustainable city policy for managing shared dockless e-scooters. *Procedia Computer Science*, 238:722–727, 2024.
- [10] Domokos Eszterg  r-Kiss, D  niel Tordai, and Julio C Lopez Lizarraga. Assessment of travel behavior related to e-scooters using a stated preference experiment. *Transportation Research Part A: Policy and Practice*, 166:389–405, 2022.
- [11] Nils Fearnley. Micromobility–regulatory challenges and opportunities. *Shaping smart mobility futures: Governance and policy instruments in times of sustainability transitions*, pages 169–186, 2020.
- [12] Naroa Coretti Sanchez, I  igo Martinez, Luis Alonso Pastor, and Kent Larson. On the simulation of shared autonomous micro-mobility. *Communications in Transportation Research*, 2:100065, 2022.
- [13] Pietro Folco, Laetitia Gauvin, Michele Tizzoni, and Michael Szell. Data-driven micromobility network planning for demand and safety. *Environment and planning B: Urban analytics and city science*, 50(8):2087–2102, 2023.
- [14] Marisdea Castiglione, Antonio Comi, Rosita De Vincintis, Andreea Dumitru, and Marialisa Nigro. Delivering in urban areas: a probabilistic-behavioral approach for forecasting the use of electric micromobility. *Sustainability*, 14(15):9075, 2022.
- [15] Aryan Hosseinzadeh, Abolfazl Karimpour, and Robert Kluger. Factors influencing shared micromobility services: An analysis of e-scooters and bikeshare. *Transportation Research Part D: Transport and Environment*, 100:103047, 2021.
- [16] Michel Geipel, Beatriz Martinez-Rico, Benjamin B  ttner, and David Duran-Rod  s. Spatial factors associated with usage of different on-demand elements within mobility hubs: a systematic literature review. *Transport Reviews*, 2024.
- [17] Aoyong Li, Kun Gao, Pengxiang Zhao, and Kay W. Axhausen. Integrating shared e-scooters as the feeder to public transit: A comparative analysis of 124 european cities. *Transportation Research Part C: Emerging Technologies*, 160:104496, 2024.
- [18] J  rgen Aarhaug, Nils Fearnley, and Espen Johnsson. E-scooters and public transport – complement or competi-

- tion? *Research in Transportation Economics*, 98:101279, 2023.
- [19] Yiming Xu, Qian Ke, Xiaojian Zhang, and Xilei Zhao. Icn: Interactive convolutional network for forecasting travel demand of shared micromobility. *GeoInformatica*, pages 1–26, 2024.
- [20] Aryan Hosseinzadeh, Majeed Algomaiah, Robert Kluger, and Zhixia Li. Spatial analysis of shared e-scooter trips. *Journal of transport geography*, 92:103016, 2021.
- [21] Doosun Hong, Sunghoon Jang, and Chungwon Lee. Investigation of shared micromobility preference for last-mile travel on shared parking lots in city center. *Travel Behaviour and Society*, 30:163–177, 2023.
- [22] Jiyoung Ko and Yung-Cheol Byun. Analyzing factors affecting micro-mobility and predicting micro-mobility demand using ensemble voting regressor. *Electronics*, 12(21):4410, 2023.
- [23] Anthony Kimpton, Julia Loginova, Dorina Pojani, Richard Bean, Thomas Sigler, and Jonathan Corcoran. Weather to scoot? how weather shapes shared e-scooter ridership patterns. *Journal of Transport Geography*, 104:103439, 2022.
- [24] Giorgia Chiotti. *Exploring micromobility dynamics through Machine Learning prediction algorithms: an analysis of urban transportation patterns*. PhD thesis, Politecnico di Torino, 2023.
- [25] Kanokporn Boonjubut and Hiroshi Hasegawa. Accuracy of hourly demand forecasting of micro mobility for effective rebalancing strategies. *Management Systems in Production Engineering*, 30(3):246–252, 2022.
- [26] Seung Woo Ham, Jung-Hoon Cho, Sangwoo Park, and Dong-Kyu Kim. Spatiotemporal demand prediction model for e-scooter sharing services with latent feature and deep learning. *Transportation research record*, 2675(11):34–43, 2021.
- [27] Jia-Cherng Song, I-Yun Lisa Hsieh, and Chuin-Shan Chen. Sparse trip demand prediction for shared e-scooter using spatio-temporal graph neural networks. *Transportation research part D: transport and environment*, 125:103962, 2023.
- [28] Daniela Arias-Molinares, Yihan Xu, Benjamin Büttner, and David Duran-Rodas. Exploring key spatial determinants for mobility hub placement based on micromobility ridership. *Journal of Transport Geography*, 110:103621, 2023.
- [29] Yijia Hu, Mushu Zhao, and Zhan Zhao. Uncovering heterogeneous effects of link-level street environment on e-bike and e-scooter usage. *Transportation Research Part D: Transport and Environment*, 136:104477, 2024.
- [30] Sujae Kim, Sangho Choo, Gyeongjae Lee, and Sanghun Kim. Predicting demand for shared e-scooter using community structure and deep learning method. *Sustainability*, 14(5), 2022.
- [31] Helena Freire de Almeida, Rui J Lopes, João M Carrilho, and Sara Eloy. Unfolding the dynamical structure of lisbon’s public space: space syntax and micromobility data. *Applied network science*, 6:1–21, 2021.
- [32] Sean Taylor and Benjamin Letham. Forecasting at scale. *The American Statistician*, 72, 09 2017.
- [33] Q. Yu, B. A. Tolson, H. Shen, M. Han, J. Mai, and J. Lin. Enhancing long short-term memory (lstm)-based stream-flow prediction with a spatially distributed approach. *Hydrology and Earth System Sciences*, 28(9):2107–2122, 2024.
- [34] Dangli Wang, Yangran Meng, Shuzhe Chen, Cheng Xie, and Zhao Liu. A hybrid model for vessel traffic flow prediction based on wavelet and prophet. *Journal of Marine Science and Engineering*, 9(11), 2021.
- [35] Hao Li, Zhendong Yuan, Tessio Novack, Wei Huang, and Alexander Zipf. Understanding spatiotemporal trip purposes of urban micro-mobility from the lens of dockless e-scooter sharing. *Computers, Environment and Urban Systems*, 96:101848, 2022.
- [36] Keyvan Hosseini, Agnieszka Stefaniec, Margaret O’Mahony, and Brian Caulfield. Optimising shared electric mobility hubs: Insights from performance analysis and factors influencing riding demand. *Case Studies on Transport Policy*, 13:101052, 2023.
- [37] Scott Lundberg. A unified approach to interpreting model predictions. *arXiv preprint arXiv:1705.07874*, 2017.
- [38] Sara Hassam, Nuno Alpalhão, and Miguel de Castro Neto. A spatiotemporal comparative analysis of docked and dockless shared micromobility services. *Smart Cities*, 7(2):880–912, 2024.
- [39] Hung-Chi Liu and Jen-Jia Lin. Associations of built environments with spatiotemporal patterns of public bicycle use. *Journal of transport geography*, 74:299–312, 2019.
- [40] Chen Feng, Junfeng Jiao, and Haofeng Wang. Estimating e-scooter traffic flow using big data to support planning for micromobility. *Journal of Urban Technology*, 29, 12 2020.
- [41] Jessica Lazarus, Jean Pourquier, Frank Feng, Henry Hamel, and Susan Shaheen. Micromobility evolution and expansion: Understanding how docked and dockless bikesharing models complement and compete – a case study of san francisco. *Journal of Transport Geography*, 84:102620, 04 2020.
- [42] Daniel Rodriguez-Roman, Andrés G Camacho Bonet, Gabriela Yáñez González, Fernando A Acosta Pérez, Carlos A del Valle González, Benjamín Colucci-Ríos, and Alberto M Figueroa-Medina. Travel patterns and spatial access in a dockless e-scooter service in puerto

- rico. *Case studies on transport policy*, 10(2):915–926, 2022.
- [43] Fanchao Liao and Gonçalo Correia. Electric carsharing and micromobility: A literature review on their usage pattern, demand, and potential impacts. *International Journal of Sustainable Transportation*, 16(3):269–286, 2022.
- [44] Fuchs Sophia, Duran-Rodas David, Stöckle Michael, and Pfertner Maximilian. Who uses shared microbilty? exploring users’ social characteristics beyond sociodemographics. In *2021 7th International Conference on Models and Technologies for Intelligent Transportation Systems (MT-ITS)*, pages 1–6. IEEE, 2021.
- [45] Alexandra Bretones and Oriol Marquet. Sociopsychological factors associated with the adoption and usage of electric micromobility. a literature review. *Transport policy*, 127:230–249, 2022.
- [46] Zoi Christoforou, Anna Mariam Psarrou Kalakoni, and Nadir Farhi. Neighborhood characteristics encouraging micromobility: An observational study for tourists and local users. *Travel Behaviour and Society*, 32:100564, 2023.
- [47] Hung-Chi Liu and Jen-Jia Lin. Associations of built environments with spatiotemporal patterns of shared scooter use: A comparison with shared bike use. *Transport Policy*, 126:107–119, 2022.
- [48] Farzana Mehzabin Tuli, Suman Mitra, and Mariah B. Crews. Factors influencing the usage of shared e-scooters in chicago. *Transportation Research Part A: Policy and Practice*, 154:164–185, 2021.
- [49] Robert B Noland. Scootin’ in the rain: Does weather affect micromobility? *Transportation research part A: policy and practice*, 149:114–123, 2021.
- [50] Rui Xin, Tinghua Ai, Linfang Ding, Ruoxin Zhu, and Liqiu Meng. Impact of the covid-19 pandemic on urban human mobility-a multiscale geospatial network analysis using new york bike-sharing data. *Cities*, 126:103677, 2022.
- [51] Helinyi Peng, Yuuki Nishiyama, and Kaoru Sezaki. Assessing environmental benefits from shared micromobility systems using machine learning algorithms and monte carlo simulation. *Sustainable Cities and Society*, 87:104207, 2022.
- [52] Xiaoyang Wang, Yao Ma, Yiqi Wang, Wei Jin, Xin Wang, Jiliang Tang, Caiyan Jia, and Jian Yu. Traffic flow prediction via spatial temporal graph neural network. In *Proceedings of the web conference 2020*, pages 1082–1092, 2020.
- [53] Maren Schnieder. Ebike sharing vs. bike sharing: Demand prediction using deep neural networks and random forests. *Sustainability*, 15(18):13898, 2023.
- [54] Natalia Zuniga-Garcia, Mauricio Tec, James Scott, and Randy Machemehl. Evaluation of e-scooters as transit last-mile solution. *Transportation Research Part C: Emerging Technologies*, 139:103660, 06 2022.
- [55] Hongyi Lin, Yixu He, Shen Li, and Yang Liu. Insights into travel pattern analysis and demand prediction: A data-driven approach in bike-sharing systems. *Journal of Transportation Engineering, Part A: Systems*, 150(2):04023132, 2024.
- [56] Mark A Hall. *Correlation-based feature selection for machine learning*. PhD thesis, The University of Waikato, 1999.
- [57] Yiming Xu, Xilei Zhao, Xiaojian Zhang, and Mudit Paliwal. Real-time forecasting of dockless scooter-sharing demand: A spatio-temporal multi-graph transformer approach. *IEEE Transactions on Intelligent Transportation Systems*, 24(8):8507–8518, 2023.
- [58] Songhyeon Shin and Sangho Choo. Influence of built environment on micromobility–pedestrian accidents. *Sustainability*, 15(1):582, 2022.
- [59] Pengxiang Zhao, He Haitao, Aoyong Li, and Ali Mansourian. Impact of data processing on deriving micromobility patterns from vehicle availability data. *Transportation Research Part D: Transport and Environment*, 97:102913, 2021.
- [60] Klaus Greff, Rupesh K Srivastava, Jan Koutník, Bas R Steunebrink, and Jürgen Schmidhuber. Lstm: A search space odyssey. *IEEE transactions on neural networks and learning systems*, 28(10):2222–2232, 2016.
- [61] Rahul Dey and Fathi M Salem. Gate-variants of gated recurrent unit (gru) neural networks. In *2017 IEEE 60th international midwest symposium on circuits and systems (MWSCAS)*, pages 1597–1600. IEEE, 2017.
- [62] Adrian Hernandez, Meredith Raymer, and Ying Chen. Where did bike-share boom? analyzing impact of infrastructure lockdowns on bike-sharing in chicago. *Transportation Research Interdisciplinary Perspectives*, 23:101015, 2024.
- [63] Nadav Shalit, Michael Fire, and Eran Ben-Elia. A supervised machine learning model for imputing missing boarding stops in smart card data. *Public Transport*, 15(2):287–319, 2023.
- [64] Ofer Shahal, Itzhak Benenson, Aleksey Ogulenko, and Arik Talor. Towards a sustainable city policy for managing shared dockless e-scooters. *Procedia Computer Science*, 238:722–727, 2024. The 15th International Conference on Ambient Systems, Networks and Technologies Networks (ANT) / The 7th International Conference on Emerging Data and Industry 4.0 (EDI40), April 23-25, 2024, Hasselt University, Belgium.

- [65] Ulrik Brandes. A faster algorithm for betweenness centrality. *Journal of mathematical sociology*, 25(2):163–177, 2001.
- [66] Abraham Berman and Robert J Plemmons. *Nonnegative matrices in the mathematical sciences*. SIAM, 1994.
- [67] Abdol-Hossein Esfahanian. Connectivity algorithms. *Topics in structural graph theory*, pages 268–281, 2013.
- [68] Alain Barrat, Marc Barthélemy, Romualdo Pastor-Satorras, and Alessandro Vespignani. The architecture of complex weighted networks. *Proceedings of the national academy of sciences*, 101(11):3747–3752, 2004.
- [69] Giorgio Fagiolo. Clustering in complex directed networks. *Physical Review E—Statistical, Nonlinear, and Soft Matter Physics*, 76(2):026107, 2007.
- [70] Leo Breiman, Jerome Friedman, Richard A Olshen, and Charles J Stone. *Classification and regression trees*. Routledge, 2017.
- [71] Hui Zou and Trevor Hastie. Regularization and variable selection via the elastic net. *Journal of the Royal Statistical Society Series B: Statistical Methodology*, 67(2):301–320, 2005.
- [72] Robert Tibshirani. Regression shrinkage and selection via the lasso. *Journal of the Royal Statistical Society Series B: Statistical Methodology*, 58(1):267–288, 1996.
- [73] Arthur E Hoerl and Robert W Kennard. Ridge regression: Biased estimation for nonorthogonal problems. *Technometrics*, 12(1):55–67, 1970.
- [74] Leo Breiman. Random forests. *Machine learning*, 45:5–32, 2001.
- [75] Thomas Cover and Peter Hart. Nearest neighbor pattern classification. *IEEE transactions on information theory*, 13(1):21–27, 1967.
- [76] populusAI. Populus ai rides dataset 04/2020-02/2023. <https://www.populus.ai>, 2024.
- [77] Tel Aviv Municipality. Tel aviv open data portal. <https://opendata.tel-aviv.gov.il/>, n.d. Accessed: YYYY-MM-DD.
- [78] Edouard Mathieu, Hannah Ritchie, Lucas Rodés-Guirao, Cameron Appel, Daniel Gavrilov, Charlie Giattino, Joe Hasell, Bobbie Macdonald, Saloni Dattani, Diana Beltekian, Esteban Ortiz-Ospina, and Max Roser. Covid-19 pandemic. *Our World in Data*, 2020. <https://ourworldindata.org/coronavirus>.
- [79] Energy Institute. Oil price - crude prices since 1861. <https://ourworldindata.org/grapher/crude-oil-prices>, 2024. Data processed by Our World in Data. Accessed: 2025-01-05.
- [80] Hannah Ritchie. Google mobility trends: How has the pandemic changed the movement of people around the world? *Our World in Data*, 2020. <https://ourworldindata.org/covid-mobility-trends>.
- [81] Israeli Government. Israeli meteorological data. <https://data.gov.il/dataset/481/resource/c02e5c7d-0adb-4e04-a941-06e281180294>, n.d. Accessed: YYYY-MM-DD.
- [82] Aric Hagberg, Pieter Swart, and Daniel S Chult. Exploring network structure, dynamics, and function using networkx. Technical report, Los Alamos National Lab.(LANL), Los Alamos, NM (United States), 2008.
- [83] Chris Brunsdon, Stewart Fotheringham, and Martin Charlton. Geographically weighted regression. *Journal of the Royal Statistical Society: Series D (The Statistician)*, 47(3):431–443, 1998.
- [84] Franco Scarselli, Marco Gori, Ah Chung Tsoi, Markus Hagenbuchner, and Gabriele Monfardini. The graph neural network model. *IEEE transactions on neural networks*, 20(1):61–80, 2008.
- [85] Andrea Cini, Ivan Marisca, Filippo Maria Bianchi, and Cesare Alippi. Scalable spatiotemporal graph neural networks. In *Proceedings of the AAAI conference on artificial intelligence*, volume 37, pages 7218–7226, 2023.

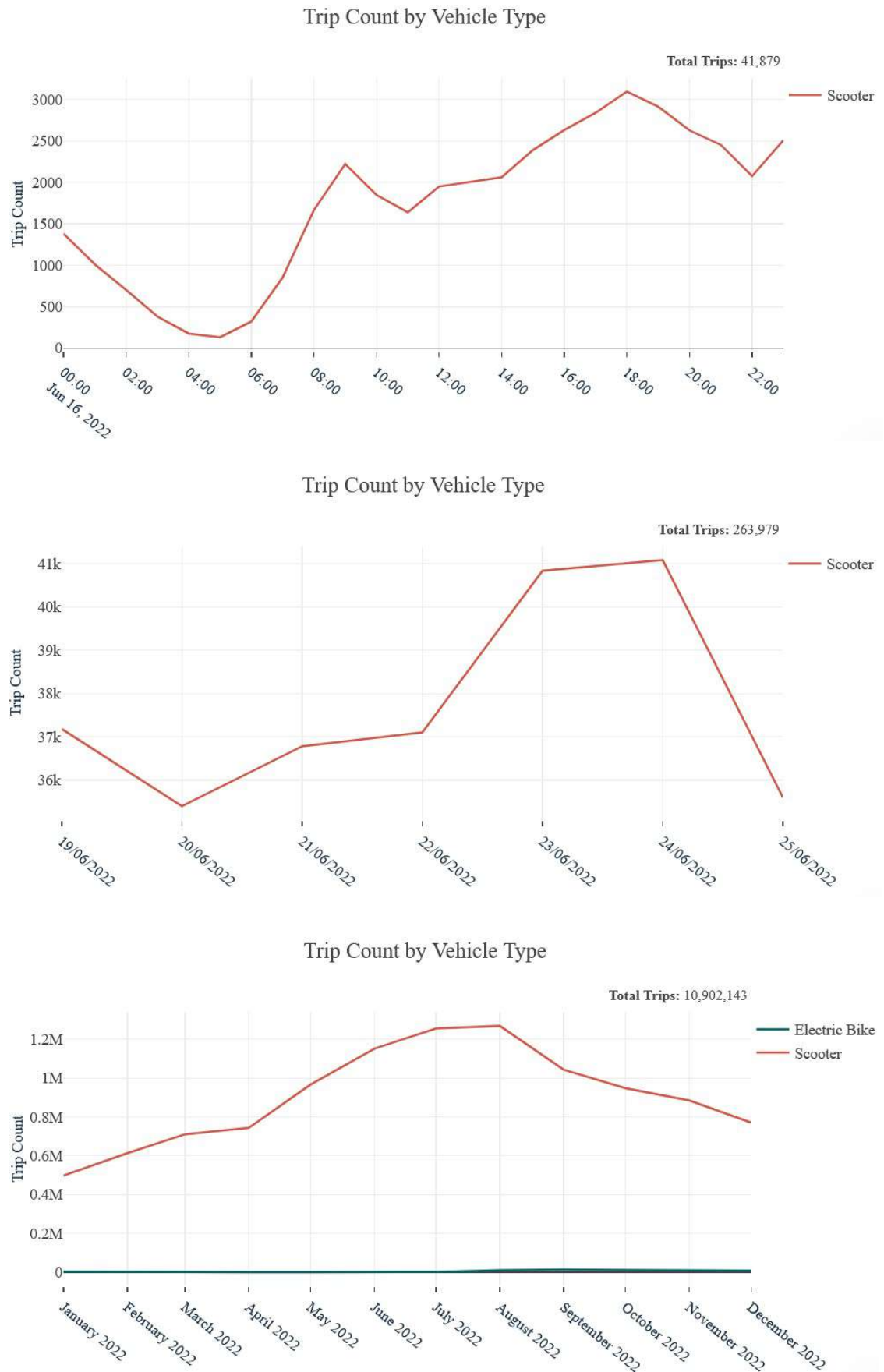


Figure 2. Hourly, Weekly and Yearly demand of Shared Micromobility in 2022

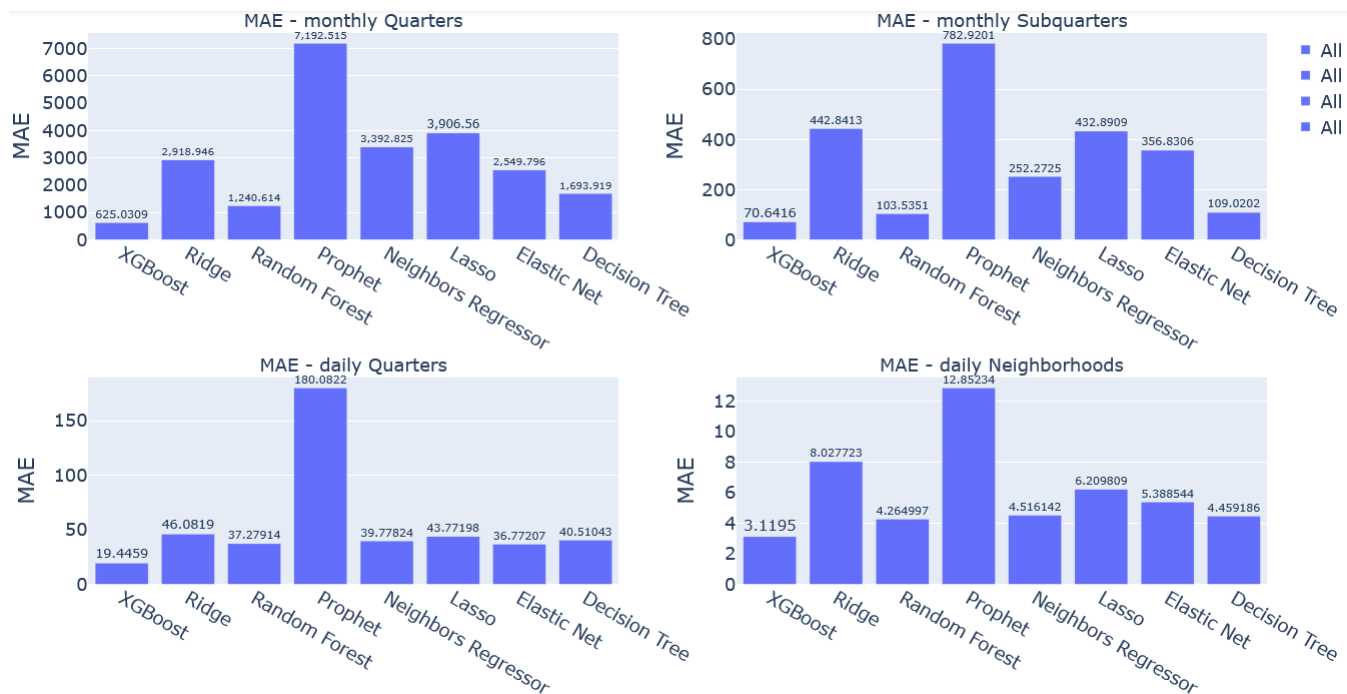


Figure 3. Comparison of MAE for various ML models, time frames and spatial divisions

Appendix

.1 Features Tables

The mean absolute error (MAE) measures the average absolute difference between the predicted and actual values. Mean Absolute Percentage Error (MAPE) - Measures errors as percentages to compare between scales. Root Mean Squared Error (RMSE)¹³¹⁴

Those are the spatial features we used:

¹³MSE: Quantifies the average squared difference between the predicted and actual values, penalizing higher deviations.

¹⁴RMSE: The square root of MSE provides an interpretable measure of error magnitude, useful for penalizing large deviations. While RMSE is sensitive to outliers, its emphasis on extensive errors makes it a valuable metric for applications where extreme mispredictions can significantly impact decision-making.

Table S2. Table of the spatial features we used in Tel Aviv[77]:

Feature	Description	Dataset
Number of Public Hosting Spaces	Total number of public areas available for hosting events or gatherings	Tel Aviv Open Data.
Number of Licensed Businesses	Total number of businesses operating with a valid license or permit	Tel Aviv Open Data.
Number of Nature Sites (2012)	Total number of designated nature sites as of 2012	Tel Aviv Open Data.
Area Owned by Municipality	Total land area owned by the city municipality	Tel Aviv Open Data.
Number of Social Services Departments	Total number of departments providing social services within the city	Tel Aviv Open Data.
Number of Public Innovation Projects	Total number of projects aimed at fostering innovation in public spaces	Tel Aviv Open Data.
Area of Building Requests and Permits	Total area for which construction requests and permits have been submitted	Tel Aviv Open Data.
Area of Construction Sites	Total area designated for ongoing construction projects	Tel Aviv Open Data.
Number of Azor VaBitzron (Support Programs)	Total number of social support programs (e.g., Azor VaBitzron)	Tel Aviv Open Data.
Number of Immigrant Absorption Centers	Total number of centers dedicated to helping new immigrants integrate into society	Tel Aviv Open Data.
Number of Rights Assistance Centers	Total number of centers assisting residents in exercising their rights (e.g., legal rights, social benefits)	Tel Aviv Open Data.
Number of Nursing Homes	Total number of nursing homes for the elderly	Tel Aviv Open Data.
Number of Day Centers for the Elderly	Total number of day centers dedicated to elderly care	Tel Aviv Open Data.
Number of Senior Citizen Clubs	Total number of social clubs for senior citizens	Tel Aviv Open Data.
Number of Disability Institutions	Total number of institutions offering services and support to people with disabilities	Tel Aviv Open Data.
Number of Public Toilets	Total number of public toilet facilities	Tel Aviv Open Data.
Number of Drinking Fountains	Total number of public drinking fountains	Tel Aviv Open Data.
Number of Dog Parks	Total number of parks designated for dog exercise and play	Tel Aviv Open Data.
Number of Street Cat Feeding Stations	Total number of designated feeding stations for stray cats	Tel Aviv Open Data.
Length of Ecological Corridors	Total length of designated ecological corridors aimed at preserving biodiversity	Tel Aviv Open Data.
Number of Solar-Powered Rooftops	Total number of rooftops with installed solar panels	Tel Aviv Open Data.
Number of Waste Collection Points	Total number of designated spots for the collection of green waste	Tel Aviv Open Data.
Number of Recycling Facilities	Total number of recycling facilities available in the city	Tel Aviv Open Data.
Number of Composters	Total number of composting facilities for organic waste	Tel Aviv Open Data.
Number of Underground Waste Containers	Total number of underground waste collection containers	Tel Aviv Open Data.
Number of Public Wi-Fi Points	Total number of public Wi-Fi access points in the city	Tel Aviv Open Data.

Feature	Description	Dataset
Number of Public Notice Boards	Total number of public notice boards installed throughout the city	Tel Aviv Open Data.
Number of Trees	Total number of trees in public spaces across the city	Tel Aviv Open Data.
Area of Social Welfare Zones	Total area designated for welfare-related services and facilities	Tel Aviv Open Data.
Area of Urban Nature Sites	Total area of sites designated for the preservation of urban nature	Tel Aviv Open Data.
Number of Good Deeds Day Events	Total number of community events held on Good Deeds Day, aimed at promoting social responsibility	Tel Aviv Open Data.
Metro Route M1 Area	Total area of land dedicated to the M1 metro route	Tel Aviv Open Data.
Metro Route M2 Area	Total area of land dedicated to the M2 metro route	Tel Aviv Open Data.
Metro Route M3 Area	Total area of land dedicated to the M3 metro route	Tel Aviv Open Data.
Number of Purple Line Stations	Total number of stations along the Purple Line of the light rail system	Tel Aviv Open Data.
Number of Green Line Stations	Total number of stations along the Green Line of the light rail system	Tel Aviv Open Data.
Number of Red Line Stations	Total number of stations along the Red Line of the light rail system	Tel Aviv Open Data.
Purple Line Track Area	Total land area allocated for the Purple Line track	Tel Aviv Open Data.
Green Line Track Area	Total land area allocated for the Green Line track	Tel Aviv Open Data.
Red Line Track Area	Total land area allocated for the Red Line track	Tel Aviv Open Data.
Light Rail Engineering Facilities Area	Total area dedicated to the engineering facilities for the light rail system	Tel Aviv Open Data.
Light Rail Staging Areas	Total land area used for light rail construction staging	Tel Aviv Open Data.
Number of Loading/Unloading Signs	Total number of signs designated for loading and unloading zones	Tel Aviv Open Data.
Number of Waze Reports	Total number of traffic or incident reports generated through Waze	Tel Aviv Open Data.
Length of Waze Traffic Congestion	Total length of traffic congestion areas reported via Waze	Tel Aviv Open Data.
Number of Night Parking Lots for Residents	Total number of parking lots dedicated to residents for overnight parking	Tel Aviv Open Data.
Number of Ahuzat Ha-Hof Parking Lots	Total number of parking lots managed by Ahuzat HaHof (the municipal parking authority)	Tel Aviv Open Data.
Area for Limited Access Zones for Shared Vehicles	Total area where access is restricted or regulated for shared vehicle services	Tel Aviv Open Data.
Number of Parking Spots for Micro-Mobility Vehicles	Total number of parking spaces designated for small electric vehicles (e.g., scooters)	Tel Aviv Open Data.
Length of Pedestrian-Friendly Streets	Total length of streets that prioritize pedestrian movement and walkability	Tel Aviv Open Data.
Number of AutoTel Parking Spots	Total number of parking spots reserved for AutoTel (a car-sharing service)	Tel Aviv Open Data.
Number of Tel-O-Fun Bike Stations	Total number of docking stations for the Tel-O-Fun bike-sharing program	Tel Aviv Open Data.
Number of Hop-On Charging Stations	Total number of charging stations for the Hop-On electric mobility service	Tel Aviv Open Data.
Number of Public Transit Lane Cameras	Total number of cameras monitoring lanes designated for public transit	Tel Aviv Open Data.
Number of NETZ Cameras	Total number of NETZ cameras used for traffic enforcement	Tel Aviv Open Data.

Feature	Description	Dataset
Number of Public Transit Terminals	Total number of public transit terminals	Tel Aviv Open Data.
Number of Weekend Public Transit Stations	Total number of stations where weekend public transit is available	Tel Aviv Open Data.
Length of Weekend Public Transit Lines	Total length of routes served by weekend public transit	Tel Aviv Open Data.
Number of Ministry of Transportation Bus Stops	Total number of bus stops managed by the Ministry of Transportation	Tel Aviv Open Data.
Number of Traffic Lights at Intersections	Total number of intersections with traffic lights	Tel Aviv Open Data.
Area of Night Construction - Buildings	Total area where night construction activities related to buildings are occurring	Tel Aviv Open Data.
Number of Public Parking Lots	Total number of public parking lots	Tel Aviv Open Data.
Number of Private Parking Lots	Total number of privately owned parking lots	Tel Aviv Open Data.
Area of Bubble Dan Service Zones	Total area where the Bubble Dan on-demand public transportation service operates	Tel Aviv Open Data.
Number of Loading/Unloading Pilots	Total number of pilot programs for designated loading and unloading zones	Tel Aviv Open Data.
Number of Motorcycle Parking Spaces	Total number of parking spaces allocated for motorcycles	Tel Aviv Open Data.
Number of Traffic Signs	Total number of traffic direction signs in the city	Tel Aviv Open Data.
Number of Fuel Stations	Total number of fuel stations within the city	Tel Aviv Open Data.
Number of Intersections	Total number of road intersections	Tel Aviv Open Data.
Number of Bicycle Maintenance Stations	Total number of bicycle maintenance stations throughout the city	Tel Aviv Open Data.
Length of Bicycle Lanes	Total length of designated bicycle lanes	Tel Aviv Open Data.
Length of 2025 City Bicycle Strategy	Total length of bicycle lanes planned under the city's 2025 bicycle strategy	Tel Aviv Open Data.
Length of Bicycle Strategy Execution Status	Total length of bicycle lanes that have been completed as part of the 2025 strategy	Tel Aviv Open Data.
Length of the Ophnidan (Bicycle Highway)	Total length of the Ophnidan, a high-speed bicycle route designed for urban commuting	Tel Aviv Open Data.
Length of Bridges	Total length of bridges in the city	Tel Aviv Open Data.
Length of Public Transit Lanes	Total length of dedicated public transit lanes	Tel Aviv Open Data.
Area of Vehicle Towing Zones	Total area where vehicles are towed due to illegal parking or other violations	Tel Aviv Open Data.
Area of Parking Zones	Total area designated for public parking	Tel Aviv Open Data.
Number of Defibrillators	Total number of publicly available defibrillators	Tel Aviv Open Data.
Number of Medical Institutions	Total number of medical institutions, including hospitals and clinics	Tel Aviv Open Data.
Number of Health Clinics	Total number of general health clinics in the city	Tel Aviv Open Data.
Number of Pharmacies	Total number of pharmacies	Tel Aviv Open Data.
Number of Tipat Halav Clinics	Total number of Tipat Halav (maternal and child health) clinics	Tel Aviv Open Data.
Number of Mental Health Services	Total number of mental health facilities and services	Tel Aviv Open Data.
Number of Magen David Adom Stations	Total number of emergency stations operated by Magen David Adom	Tel Aviv Open Data.
Number of Educational Psychological Services	Total number of stations offering educational psychological services	Tel Aviv Open Data.

Feature	Description	Dataset
Area of Traffic Noise Levels (4 meters)	Total area exposed to traffic noise at a height of 4 meters above ground level	Tel Aviv Open Data.
Area of Traffic Noise Levels (45 meters)	Total area exposed to traffic noise at a height of 45 meters above ground level	Tel Aviv Open Data.
Number of Cell Towers Under Construction	Total number of cellular towers that are under construction	Tel Aviv Open Data.
Number of Operational Cell Towers	Total number of fully operational cellular towers	Tel Aviv Open Data.
Number of Tashpe Schools (Elementary)	Total number of elementary schools categorized as Tashpe (state-religious)	Tel Aviv Open Data.
Number of Tashpad Schools (Elementary)	Total number of elementary schools categorized as Tashpad (state-secular)	Tel Aviv Open Data.
Number of Tashpe Kindergartens	Total number of kindergartens categorized as Tashpe (state-religious)	Tel Aviv Open Data.
Number of Tashpad Kindergartens	Total number of kindergartens categorized as Tashpad (state-secular)	Tel Aviv Open Data.
Number of Youth Clubs	Total number of youth clubs	Tel Aviv Open Data.
Number of Recognized Daycares	Total number of officially recognized early childhood daycare centers	Tel Aviv Open Data.
Number of School District Labels (Tashpe)	Total number of school district labels for Tashpe schools	Tel Aviv Open Data.
Number of School District Labels (Tashpad)	Total number of school district labels for Tashpad schools	Tel Aviv Open Data.
Number of General School District Labels	Total number of school district labels for general schools	Tel Aviv Open Data.
Number of State School District Labels	Total number of school district labels for state schools	Tel Aviv Open Data.
Number of Religious School District Labels	Total number of school district labels for religious schools	Tel Aviv Open Data.
Number of Arab School District Labels	Total number of school district labels for Arab schools	Tel Aviv Open Data.
Number of Synagogues	Total number of synagogues	Tel Aviv Open Data.
Number of Mikvahs (Ritual Baths)	Total number of mikvahs (ritual baths)	Tel Aviv Open Data.
Number of Cemeteries	Total number of cemeteries	Tel Aviv Open Data.
Number of Other Religious Institutions	Total number of religious institutions other than synagogues or cemeteries	Tel Aviv Open Data.
Area of Eruv Lines	Total length or area covered by Eruv lines (boundaries for religious purposes)	Tel Aviv Open Data.
Number of Tourist Offices	Total number of tourist information centers or offices	Tel Aviv Open Data.
Number of ATMs	Total number of ATMs (automated teller machines)	Tel Aviv Open Data.
Number of Bank Branches	Total number of bank branches	Tel Aviv Open Data.
Beach Area	Total area designated as beach property	Tel Aviv Open Data.
Green Space Area and Public Parks	Total area of green spaces and public parks	Tel Aviv Open Data.
Number of Embassies	Total number of embassies	Tel Aviv Open Data.
Number of Hotels	Total number of hotels	Tel Aviv Open Data.
Number of Playgrounds	Total number of playgrounds for children	Tel Aviv Open Data.
Number of Community Gardens	Total number of community gardens	Tel Aviv Open Data.

Feature	Description	Dataset
Number of Water Fountains	Total number of water fountains	Tel Aviv Open Data.
Number of Table Tennis Facilities in Parks	Total number of table tennis facilities located in public parks	Tel Aviv Open Data.
Number of Playrooms	Total number of indoor playrooms for children	Tel Aviv Open Data.
Number of Fountains	Total number of public fountains	Tel Aviv Open Data.
Number of Community Institutions	Total number of community institutions	Tel Aviv Open Data.
Number of Post Offices	Total number of post offices	Tel Aviv Open Data.
Number of Stadiums and Sports Halls	Total number of stadiums and sports halls	Tel Aviv Open Data.
Number of Gyms	Total number of gyms or fitness centers	Tel Aviv Open Data.
Number of Sports Halls	Total number of indoor sports halls	Tel Aviv Open Data.
Number of Swimming Pools	Total number of public swimming pools	Tel Aviv Open Data.
Number of Sports Fields	Total number of outdoor sports fields	Tel Aviv Open Data.
Number of Fitness Facilities in Parks	Total number of fitness facilities located in public parks	Tel Aviv Open Data.
Number of Beach and Ocean Sports Facilities	Total number of sports facilities located on the beach or in the ocean	Tel Aviv Open Data.
Number of Donation Benches	Total number of benches designated for charitable purposes (e.g., benches with plaques recognizing donations)	Tel Aviv Open Data.
Number of Special Trees	Total number of trees designated as special or protected	Tel Aviv Open Data.
Number of This-Is-The-Place Sites	Total number of sites designated under ""This-Is-The-Place"" for historical or cultural reasons	Tel Aviv Open Data.
Number of Youth Movements	Total number of youth movements or organizations	Tel Aviv Open Data.
Number of Young Adult and Entrepreneurship Centers	Total number of centers focused on young adults and entrepreneurship	Tel Aviv Open Data.
Number of Dance Centers	Total number of centers focused on dance or performing arts	Tel Aviv Open Data.
Number of Libraries	Total number of public libraries	Tel Aviv Open Data.
Number of Outdoor Libraries	Total number of outdoor libraries	Tel Aviv Open Data.
Number of Memorials	Total number of memorials or monuments	Tel Aviv Open Data.
Number of Museums	Total number of museums	Tel Aviv Open Data.
Number of Art Galleries	Total number of art galleries	Tel Aviv Open Data.
Number of Theaters	Total number of theaters or performance spaces	Tel Aviv Open Data.
Number of Cinemas	Total number of movie theaters	Tel Aviv Open Data.
Number of Music Centers	Total number of centers focused on music education or performance	Tel Aviv Open Data.
Number of Auditoriums	Total number of auditoriums	Tel Aviv Open Data.
Area of Sustainable Neighborhoods	Total area of neighborhoods classified as sustainable or eco-friendly	Tel Aviv Open Data.
Number of Green Schools	Total number of schools certified as green or eco-friendly	Tel Aviv Open Data.
Length of Tel Aviv Marathon (42.2 km)	Total length of the Tel Aviv marathon route (42.2 kilometers)	Tel Aviv Open Data.

Table S3. Table of the spatial features we used in the methods:

Feature	Description	Dataset
Number of Public Hosting Spaces	Total number of public areas available for hosting events or gatherings	Open GIS layers Datasets.
Number of Licensed Businesses	Total number of businesses operating with a valid license or permit	Open GIS layers Datasets.
Number of Nature Sites	Total number of designated nature sites	Open GIS layers Datasets.
Area Owned by Municipality	Total land area owned by the city municipality	Open GIS layers Datasets.
Number of Social Services Departments	Total number of departments providing social services within the city	Open GIS layers Datasets.
Number of Public Innovation Projects	Total number of projects aimed at fostering innovation in public spaces	Open GIS layers Datasets.
Area of Building Requests and Permits	Total area for which construction requests and permits have been submitted	Open GIS layers Datasets.
Area of Construction Sites	Total area designated for ongoing construction projects	Open GIS layers Datasets.
Number of Immigrant Absorption Centers	Total number of centers dedicated to helping new immigrants integrate into society	Open GIS layers Datasets.
Number of Rights Assistance Centers	Total number of centers assisting residents in exercising their rights (e.g., legal rights, social benefits)	Open GIS layers Datasets.
Number of Nursing Homes	Total number of nursing homes for the elderly	Open GIS layers Datasets.
Number of Day Centers for the Elderly	Total number of day centers dedicated to elderly care	Open GIS layers Datasets.
Number of Public Toilets	Total number of public toilet facilities	Open GIS layers Datasets.
Number of Drinking Fountains	Total number of public drinking fountains	Open GIS layers Datasets.
Number of Dog Parks	Total number of parks designated for dog exercise and play	Open GIS layers Datasets.
Number of Street Cat Feeding Stations	Total number of designated feeding stations for stray cats	Open GIS layers Datasets.
Length of Ecological Corridors	Total length of designated ecological corridors aimed at preserving biodiversity	Open GIS layers Datasets.
Number of Solar-Powered Rooftops	Total number of rooftops with installed solar panels	Open GIS layers Datasets.
Number of Waste Collection Points	Total number of designated spots for the collection of green waste	Open GIS layers Datasets.
Number of Recycling Facilities	Total number of recycling facilities available in the city	Open GIS layers Datasets.
Number of Composters	Total number of composting facilities for organic waste	Open GIS layers Datasets.
Number of Underground Waste Containers	Total number of underground waste collection containers	Open GIS layers Datasets.
Number of Public Wi-Fi Points	Total number of public Wi-Fi access points in the city	Open GIS layers Datasets.
Number of Public Notice Boards	Total number of public notice boards installed throughout the city	Open GIS layers Datasets.
Number of Trees	Total number of trees in public spaces across the city	Open GIS layers Datasets.

Feature	Description	Dataset
Area of Social Welfare Zones	Total area designated for welfare-related services and facilities	Open GIS layers Datasets.
Area of Urban Nature Sites	Total area of sites designated for the preservation of urban nature	Open GIS layers Datasets.
Metro Route Area	Total area of land dedicated to the metro	Open GIS layers Datasets.
Light Rail Engineering Facilities Area	Total area dedicated to the engineering facilities for the light rail system	Open GIS layers Datasets.
Light Rail Staging Areas	Total land area used for light rail construction staging	Open GIS layers Datasets.
Number of Loading/Unloading Signs	Total number of signs designated for loading and unloading zones	Open GIS layers Datasets.
Area for Limited Access Zones for Shared Vehicles	Total area where access is restricted or regulated for shared vehicle services	Open GIS layers Datasets.
Number of Parking Spots for Micro-Mobility Vehicles	Total number of parking spaces designated for small electric vehicles (e.g., scooters)	Open GIS layers Datasets.
Length of Pedestrian-Friendly Streets	Total length of streets that prioritize pedestrian movement and walkability	Open GIS layers Datasets.
Number of Public Transit Terminals	Total number of public transit terminals	Open GIS layers Datasets.
Length of Weekend Public Transit Lines	Total length of routes served by weekend public transit	Open GIS layers Datasets.
Number of Ministry of Transportation Bus Stops	Total number of bus stops managed by the Ministry of Transportation	Open GIS layers Datasets.
Number of Traffic Lights at Intersections	Total number of intersections with traffic lights	Open GIS layers Datasets.
Area of Night Construction - Buildings	Total area where night construction activities related to buildings are occurring	Open GIS layers Datasets.
Number of Public Parking Lots	Total number of public parking lots	Open GIS layers Datasets.
Number of Private Parking Lots	Total number of privately owned parking lots	Open GIS layers Datasets.
Number of Motorcycle Parking Spaces	Total number of parking spaces allocated for motorcycles	Open GIS layers Datasets.
Number of Traffic Signs	Total number of traffic direction signs in the city	Open GIS layers Datasets.
Number of Fuel Stations	Total number of fuel stations within the city	Open GIS layers Datasets.
Number of Intersections	Total number of road intersections	Open GIS layers Datasets.
Number of Bicycle Maintenance Stations	Total number of bicycle maintenance stations throughout the city	Open GIS layers Datasets.
Length of Bicycle Lanes	Total length of designated bicycle lanes	Open GIS layers Datasets.
Length of Bridges	Total length of bridges in the city	Open GIS layers Datasets.
Length of Public Transit Lanes	Total length of dedicated public transit lanes	Open GIS layers Datasets.
Area of Vehicle Towing Zones	Total area where vehicles are towed due to illegal parking or other violations	Open GIS layers Datasets.

Feature	Description	Dataset
Area of Parking Zones	Total area designated for public parking	Open GIS layers Datasets.
Number of Medical Institutions	Total number of medical institutions, including hospitals and clinics	Open GIS layers Datasets.
Number of Health Clinics	Total number of general health clinics in the city	Open GIS layers Datasets.
Number of Pharmacies	Total number of pharmacies	Open GIS layers Datasets.
Number of Mental Health Services	Total number of mental health facilities and services	Open GIS layers Datasets.
Emergency stations Stations	Total number of emergency stations	Open GIS layers Datasets.
Number of Educational Psychological Services	Total number of stations offering educational psychological services	Open GIS layers Datasets.
Number of Youth Clubs	Total number of youth clubs	Open GIS layers Datasets.
Number of Recognized Daycares	Total number of officially recognized early childhood daycare centers	Open GIS layers Datasets.
Number of General School District Labels	Total number of school district labels for general schools	Open GIS layers Datasets.
Number of State School District Labels	Total number of school district labels for state schools	Open GIS layers Datasets.
Number of ATMs	Total number of ATMs (automated teller machines)	Open GIS layers Datasets.
Number of Bank Branches	Total number of bank branches	Open GIS layers Datasets.
Beach Area	Total area designated as beach property	Open GIS layers Datasets.
Number of Embassies	Total number of embassies	Open GIS layers Datasets.
Number of Hotels	Total number of hotels	Open GIS layers Datasets.
Number of Playgrounds	Total number of playgrounds for children	Open GIS layers Datasets.
Number of Community Gardens	Total number of community gardens	Open GIS layers Datasets.
Number of Water Fountains	Total number of water fountains	Open GIS layers Datasets.
Number of Table Tennis Facilities in Parks	Total number of table tennis facilities located in public parks	Open GIS layers Datasets.
Number of Playrooms	Total number of indoor playrooms for children	Open GIS layers Datasets.
Number of Fountains	Total number of public fountains	Open GIS layers Datasets.
Number of Community Institutions	Total number of community institutions	Open GIS layers Datasets.
Number of Post Offices	Total number of post offices	Open GIS layers Datasets.
Number of Stadiums and Sports Halls	Total number of stadiums and sports halls	Open GIS layers Datasets.
Number of Gyms	Total number of gyms or fitness centers	Open GIS layers Datasets.

Feature	Description	Dataset
Number of Sports Halls	Total number of indoor sports halls	Open GIS layers Datasets.
Number of Swimming Pools	Total number of public swimming pools	Open GIS layers Datasets.
Number of Sports Fields	Total number of outdoor sports fields	Open GIS layers Datasets.
Number of Fitness Facilities in Parks	Total number of fitness facilities located in public parks	Open GIS layers Datasets.
Number of Beach and Ocean Sports Facilities	Total number of sports facilities located on the beach or in the ocean	Open GIS layers Datasets.
Number of Youth Movements	Total number of youth movements or organizations	Open GIS layers Datasets.
Number of Young Adult and Entrepreneurship Centers	Total number of centers focused on young adults and entrepreneurship	Open GIS layers Datasets.
Number of Dance Centers	Total number of centers focused on dance or performing arts	Open GIS layers Datasets.
Number of Libraries	Total number of libraries	Open GIS layers Datasets.
Number of Memorials	Total number of memorials or monuments	Open GIS layers Datasets.
Number of Museums	Total number of museums	Open GIS layers Datasets.
Number of Art Galleries	Total number of art galleries	Open GIS layers Datasets.
Number of Theaters	Total number of theaters or performance spaces	Open GIS layers Datasets.
Number of Cinemas	Total number of movie theaters	Open GIS layers Datasets.
Number of Music Centers	Total number of centers focused on music education or performance	Open GIS layers Datasets.
Number of Auditoriums	Total number of auditoriums	Open GIS layers Datasets.
Area of Neighborhoods	Total area of neighborhoods	Open GIS layers Datasets.
Number of Schools	Total number of schools	Open GIS layers Datasets.

Those are the temporal features we used:

Table S4. Table of the temporal features we used [78, 80, 79]:

Feature	Description	Dataset
Total cases	The cumulative number of COVID-19 cases in a given geographic region	COVID-19.
New cases	The number of new COVID-19 cases reported in the last time period	COVID-19.
New cases smoothed	A smoothed representation of new COVID-19 cases to account for reporting variations	COVID-19.
Total deaths	The cumulative number of deaths attributed to COVID-19	COVID-19.
New deaths	The number of new COVID-19-related deaths reported in the last time period	COVID-19.
New deaths smoothed	A smoothed representation of new deaths to account for reporting variations	COVID-19.
Total cases per million	The cumulative number of COVID-19 cases per million people in the population	COVID-19.
New cases per million	The number of new COVID-19 cases per million people in the population	COVID-19.
New cases smoothed per million	A smoothed representation of new cases per million people	COVID-19.
Total deaths per million	The cumulative number of deaths per million people in the population	COVID-19.
New deaths per million	The number of new COVID-19 deaths per million people	COVID-19.
New deaths smoothed per million	A smoothed representation of new deaths per million people	COVID-19.
Reproduction rate	The effective reproduction number (R), representing how many people one infected person will infect	COVID-19.
ICU patients	The number of patients currently in intensive care units due to COVID-19	COVID-19.
ICU patients per million	The number of ICU patients per million people in the population	COVID-19.
Hospital patients	The number of COVID-19 patients currently hospitalized	COVID-19.
Hospital patients per million	The number of hospitalized COVID-19 patients per million people	COVID-19.
Weekly ICU admissions	The number of new ICU admissions over the past week	COVID-19.
Weekly ICU admissions per million	The number of new ICU admissions per million people over the past week	COVID-19.
Weekly hospital admissions	The number of new hospital admissions over the past week	COVID-19.
Weekly hospital admissions per million	The number of new hospital admissions per million people over the past week	COVID-19.
Total tests	The cumulative number of COVID-19 tests performed	COVID-19.
New tests	The number of new COVID-19 tests conducted during the last time period	COVID-19.
Total tests per thousand	The cumulative number of COVID-19 tests per thousand people in the population	COVID-19.
New tests per thousand	The number of new COVID-19 tests per thousand people in the population	COVID-19.
New tests smoothed	A smoothed representation of new tests to account for reporting variations	COVID-19.
New tests smoothed per thousand	A smoothed representation of new tests per thousand people	COVID-19.
Positive rate	The percentage of COVID-19 tests that return a positive result	COVID-19.
Tests per case	The number of tests conducted for each reported COVID-19 case	COVID-19.

Feature	Description	Dataset
Total vaccinations	The cumulative number of COVID-19 vaccinations administered	COVID-19.
People vaccinated	The number of people who have received at least one dose of the COVID-19 vaccine	COVID-19.
People fully vaccinated	The number of people who have received all doses required to be considered fully vaccinated	COVID-19.
Total boosters	The total number of COVID-19 booster doses administered	COVID-19.
New vaccinations	The number of new COVID-19 vaccinations administered in the last time period	COVID-19.
New vaccinations smoothed	A smoothed representation of new vaccinations to account for reporting variations	COVID-19.
Total vaccinations per hundred	The cumulative number of COVID-19 vaccinations administered per hundred people in the population	COVID-19.
People vaccinated per hundred	The number of people who have received at least one dose of the vaccine per hundred people in the population	COVID-19.
People fully vaccinated per hundred	The number of fully vaccinated people per hundred people in the population	COVID-19.
Total boosters per hundred	The number of booster doses administered per hundred people in the population	COVID-19.
New vaccinations smoothed per million	A smoothed representation of new vaccinations per million people	COVID-19.
New people vaccinated smoothed	A smoothed representation of new people vaccinated	COVID-19.
New people vaccinated smoothed per hundred	A smoothed representation of new people vaccinated per hundred people in the population	COVID-19.
Stringency index	A composite measure of the severity of government-imposed COVID-19 measures, such as lockdowns and travel restrictions	COVID-19.
Handwashing facilities	The availability of handwashing facilities in a region, important for COVID-19 mitigation	COVID-19.
Excess mortality cumulative absolute	The total number of deaths above what would normally be expected during the pandemic	COVID-19.
Excess mortality cumulative	The percentage increase in mortality above what would be expected during the pandemic	COVID-19.
Excess mortality	The number of deaths above the expected number during a specific period	COVID-19.
Excess mortality cumulative per million	The number of excess deaths per million people	COVID-19.

Those are the network features we used:

Table S5. Table of the network features we used[76, 82]:

Feature	Description	Dataset
Degree centrality	The degree centrality for a node v is the fraction of nodes it is connected to.	Network data.
In degree centrality	The in-degree centrality for a node v is the fraction of nodes its incoming edges are connected to.	Network data.
Out degree centrality	The out-degree centrality for a node v is the fraction of nodes its outgoing edges are connected to.	Network data.
Betweenness centrality	Betweenness centrality of a node is the sum of the fraction of all-pairs shortest paths that pass through	Network data.
In degree	The node in_{deg} is the number of edges pointing to the node. The weighted node degree is the sum of the edge weights for edges incident to that node.	Network data.
Out degree	The node out_{deg} is the number of edges pointing out of the node. The weighted node degree is the sum of the edge weights for edges incident to that node.	Network data.
Edge betweenness	Betweenness centrality of an edge is the sum of the fraction of all-pairs shortest paths that pass through the edge	Network data.
Shortest paths length	Compute shortest path lengths in the graph.	Network data.
Number of nodes	Returns the number of nodes in the graph.	Network data.
Number of edges	Returns the number of edges between two nodes.	Network data.
Average Degree	Compute the average degree connectivity of graph. The average degree connectivity is the average nearest neighbor degree of nodes with degree k . For weighted graphs, an analogous measure can be computed using the weighted average neighbors degree defined in [1], for a node i , as where s_i is the weighted degree of node i , w_{ij} is the weight of the edge that links i and j , and $N(i)$ are the neighbors of node i .	Network data.
Average clustering	Compute the average clustering coefficient for the graph G . The clustering coefficient for the graph is the average, where is the number of nodes in G .	Network data.

.2 Prediction Results

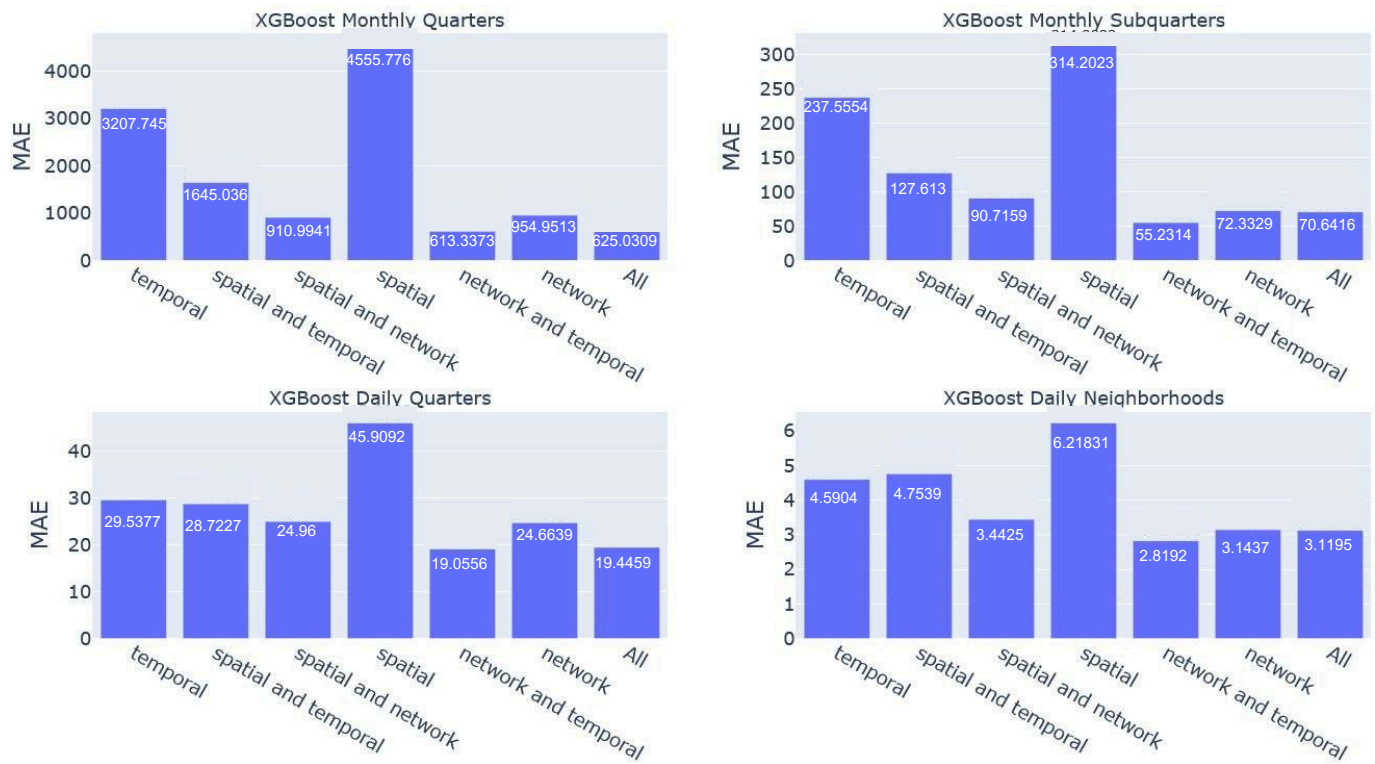


Figure S4. XGBoost Partial Features Groups MAE Comparison

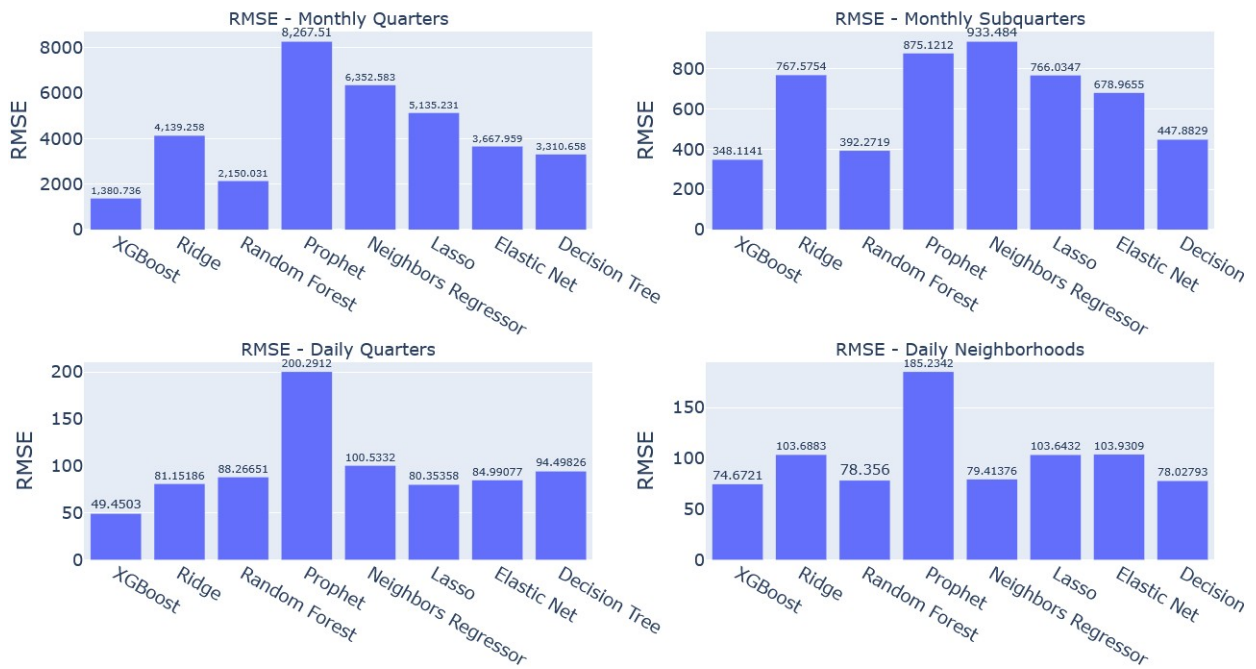


Figure S5. Comparison of RMSE for various ML models, time frames and spatial divisions

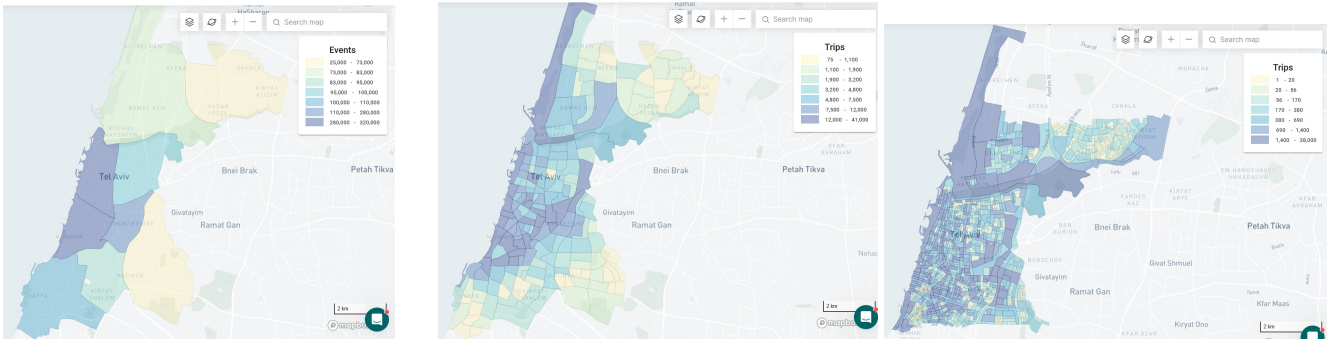


Figure S6. Shared Micromobility Trip Origins in June 2022 By Quarters, Statistical Areas and City Blocks



Figure S7. XGBoost Partial Features Groups MAE Comparison

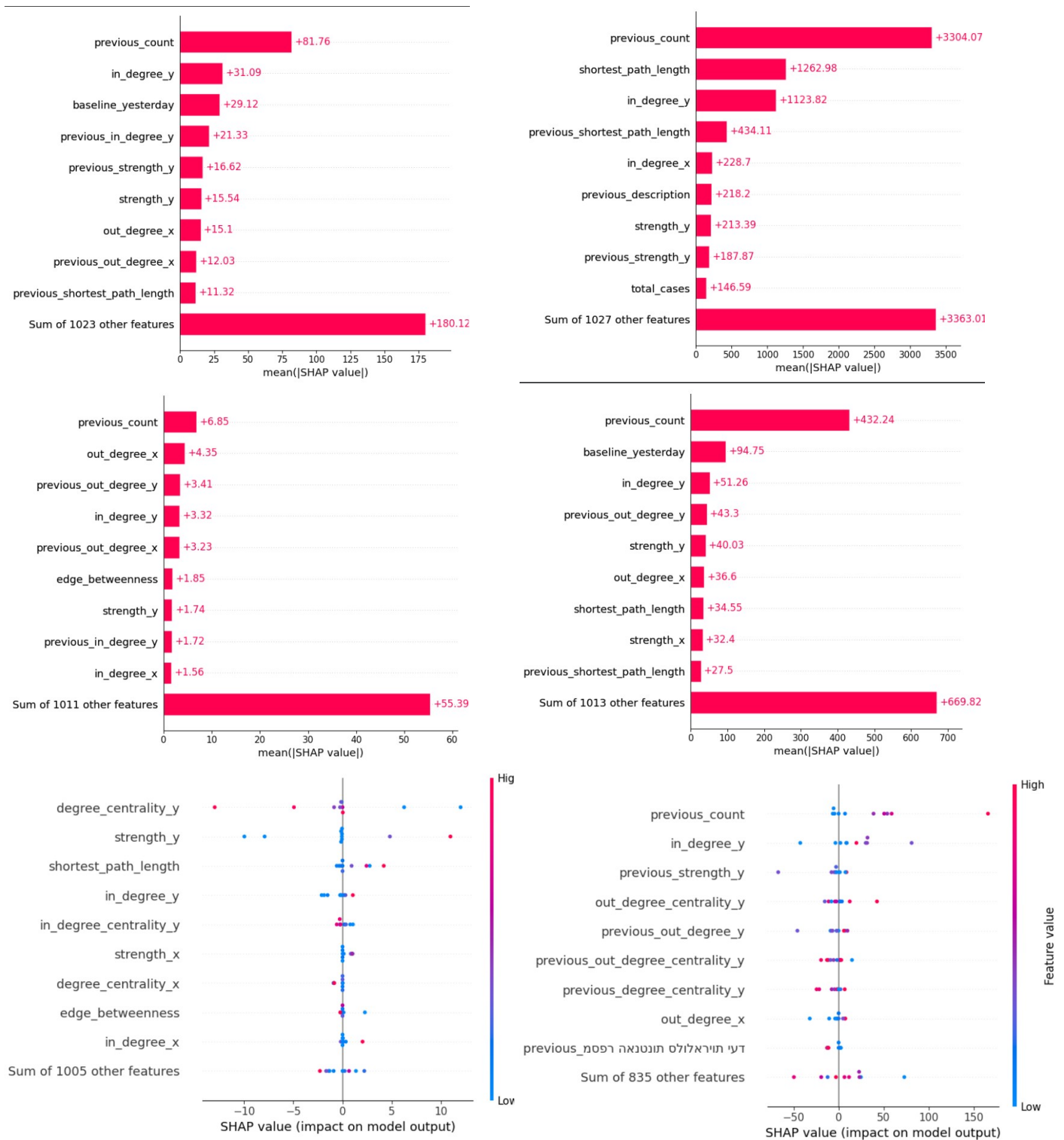


Figure S8. SHAP 10 Features Analysis Over Neighborhoods, Subquarters, Quarters over Monthly and Daily Time Frames

Table S6. Table of the results of our models over all features:

:

<i>timeframe</i>	<i>geography</i>	<i>featuretypes</i>	<i>regressortype</i>	<i>regressor</i>	<i>mae</i>	<i>mape</i>	<i>mse</i>	<i>rmse</i>
monthly	Quarters	All	Classical ML	Linear Regression	1.580e+12	1.705e+10	4.510e+24	2.120e+12
				Ridge	2918.95	18.97	1.713e+07	4139.26
				Lasso	3906.56	25.36	2.637e+07	5135.23
				Elastic Net	2549.8	14.12	1.345e+07	3667.96
				Decision Tree	1693.92	6.58	1.096e+07	3310.66
				Random Forest	1240.61	4.75	4.623e+06	2150.03
				XGBoost	625.03	0.598	1.906e+06	1380.74
				Neighbors	3392.83	6.36	4.036e+07	6352.58
				Regressor				
				Prophet	7192.5	42.8	2.733e+08	8267.51
monthly	Subquarters	All	Classical ML	Linear Regression	5.250e+11	6.176e+10	4.510e+23	6.720e+11
				Ridge	442.84	47.39	5.892e+05	767.58
				Lasso	432.89	44.97	5.868e+05	766.03
				Elastic Net	356.83	32.09	4.610e+05	678.97
				Decision Tree	109.02	3.83	2.006e+05	447.88
				Random Forest	103.54	4	1.539e+05	392.27
				XGBoost	70.6416	3.98	1.21e+05	348.11
				Neighbors	252.27	7.95	8.714e+05	933.48
				Regressor				
				Prophet	97.41	35.1	4.897e+06	875.12
monthly	Neighborhoods	All	Classical ML	Linear Regression	4.600e+11	1.490e+11	3.970e+23	6.300e+11
				Ridge	164	38.4	2.105e+05	458.77
				Lasso	154.29	34.87	2.081e+05	456.14
				Elastic Net	118.64	24.96	1.561e+05	395.08
				Decision Tree	52.96	6.44	1.226e+05	350.1
				Random Forest	47.68	6.36	1.008e+05	317.44
				XGBoost	24.92	1.44	6.601e+04	256.92
				Neighbors	68.41	6.51	1.986e+05	445.64
				Regressor				
				Prophet	164.004	26.54	3.481e+05	590.117
monthly	Statistical Areas	All	Classical ML	Linear Regression	1764.6	1753.39	6.311e+09	7.944e+04
				Ridge	13.52	2.29	1363.51	36.93
				Lasso	11.09	1.85	1299.41	36.05
				Elastic Net	13.91	1.94	3341.84	57.81
				Decision Tree	8.13	0.6	1109.27	33.31
				Random Forest	6.77	0.57	487.16	22.07
				XGBoost	3.486	0.247	422.17	20.55

Continued on next page

<i>timeframe</i>	<i>geography</i>	<i>featuretypes</i>	<i>regressortype</i>	<i>regressor</i>	<i>mae</i>	<i>mape</i>	<i>mse</i>	<i>rmse</i>
daily	Quarters	All	Classical ML	Neighbors Regressor	14.44	1.27	6009.53	77.52
				Prophet	35.8	12.32	9543.562	97.69
				Linear Regression	2.704e+10	3.463e+09	1.300e+21	3.602e+10
				Ridge	46.08	3.25	6585.62	81.15
				Lasso	43.77	2.84	6456.7	80.35
				Elastic Net	36.77	1.34	7223.43	84.99
				Decision Tree	40.51	1.16	8929.92	94.5
				Random Forest	37.28	1.14	7790.98	88.27
				XGBoost	19.44	0.507	2445.33	49.45
				Neighbors Regressor	39.78	0.72	1.011e+04	100.53
daily	Subquarters	All	Classical ML	Prophet	180.082	21.11	102079.31	200.29
				Linear Regression	1.125e+08	4.673e+07	2.150e+16	1.467e+08
				Ridge	9.11	2.65	451.79	21.26
				Lasso	7.63	1.86	441.69	21.02
				Elastic Net	6.83	1.36	459.09	21.43
				Decision Tree	5.94	0.56	584.97	24.19
				Random Forest	5.64	0.53	468.61	21.65
				XGBoost	5.16	0.71	413.57	20.34
				Prophet	19.55	8.77	1840.966	22.47
daily	Neighborhoods	All	Classical ML	Linear Regression	1.250e+06	6.973e+05	2.940e+12	1.715e+06
				Ridge	8.03	3.51	1.075e+04	103.69
				Lasso	6.21	2.33	1.074e+04	103.64
				Elastic Net	5.39	1.91	1.080e+04	103.93
				Decision Tree	4.46	0.91	6088.36	78.03
				Random Forest	4.26	0.92	6139.66	78.36
				XGBoost	3.12	0.624	5575.92	74.67
				Neighbors Regressor	4.52	1.02	6306.55	79.41
				Prophet	4.52	1.02	6306.55	79.41

.3 XGBoost Partial Feature Groups Results

Table S7. Table of the results of partial feature groups over best-performing model (XGBoost):

<i>timeframe</i>	<i>geography</i>	<i>featuretypes</i>	<i>regressortype</i>	<i>regressor</i>	<i>mae</i>	<i>mape</i>	<i>mse</i>	<i>rmse</i>
monthly	Quarters	All	Classical ML	XGBoost	625.0309	0.5967	1906432.09	1380.7361
		spatial	Classical ML	XGBoost	4555.7764	5.5012	63662425.88	7978.8737
		temporal	Classical ML	XGBoost	3207.7452	3.6127	57894962.36	7608.8739
		network	Classical ML	XGBoost	954.9513	1.0553	3676929.703	1917.5322
		spatial and temporal	Classical ML	XGBoost	1645.0361	2.0752	10445381.18	3231.9315
		network and temporal	Classical ML	XGBoost	613.3373	0.6873	1790536.491	1338.1093
		spatial and network	Classical ML	XGBoost	910.9941	0.9008	3184056.115	1784.3924
monthly	Subquarters	All	Classical ML	XGBoost	70.6416	3.98	121183.3971	348.1141
		spatial	Classical ML	XGBoost	314.2023	14.8464	750338.9533	866.2211
		temporal	Classical ML	XGBoost	237.5554	8.3583	866002.2617	930.5924
		network	Classical ML	XGBoost	72.3329	2.2271	92100.4992	303.4806
		spatial and temporal	Classical ML	XGBoost	127.613	5.5736	250538.7936	500.5385
		network and temporal	Classical ML	XGBoost	55.2314	1.5551	74634.9678	273.194
		spatial and network	Classical ML	XGBoost	90.7159	3.7254	116343.9054	341.0922
monthly	Statistical Areas	All	Classical ML	XGBoost	3.486	0.2469	422.1716	20.5468
		spatial	Classical ML	XGBoost	24.3498	2.4042	9730.4518	98.6431
		temporal	Classical ML	XGBoost	16.7209	2.1285	7109.0813	84.3154
		network	Classical ML	XGBoost	4.1727	0.249	416.2324	20.4018
		spatial and temporal	Classical ML	XGBoost	9.6455	1.367	563.0135	23.7279
		network and temporal	Classical ML	XGBoost	3.3511	0.1664	349.6717	18.6995
		spatial and network	Classical ML	XGBoost	4.6	0.3619	506.6839	22.5096
daily	Quarters	All	Classical ML	XGBoost	19.4459	0.5078	2445.331	49.4503
		spatial	Classical ML	XGBoost	45.9092	1.0286	11290.7471	106.2579
		temporal	Classical ML	XGBoost	29.5377	0.6006	7009.5826	83.7232
		network	Classical ML	XGBoost	24.6639	0.5146	3908.3447	62.5168

Continued on next page

<i>timeframe</i>	<i>geography</i>	<i>featuretypes</i>	<i>regressortype</i>	<i>regressor</i>	<i>mae</i>	<i>mape</i>	<i>mse</i>	<i>rmse</i>
		spatial and temporal	Classical ML	XGBoost	28.7227	0.8507	4981.7259	70.5813
		network and temporal	Classical ML	XGBoost	19.0556	0.4705	2317.8549	48.1441
		spatial and network	Classical ML	XGBoost	24.96	0.5635	4049.8929	63.6388
daily	Subquarters	All	Classical ML	XGBoost	5.16	0.71	413.57	20.34
daily	Neighbor-hoods	All	Classical ML	XGBoost	3.1195	0.624	5575.9221	74.6721
		spatial	Classical ML	XGBoost	6.218	1.8231	6308.4083	79.4255
		temporal	Classical ML	XGBoost	4.5904	1.2039	6312.4933	79.4512
		network	Classical ML	XGBoost	3.1437	0.5348	5238.0721	72.3745
		spatial and temporal	Classical ML	XGBoost	4.7539	1.4941	6128.2315	78.283
		network and temporal	Classical ML	XGBoost	2.8192	0.5038	5664.2666	75.2613
		spatial and network	Classical ML	XGBoost	3.4425	0.7006	5349.6342	73.1412